Syngeneic natural killer cell therapy activates dendritic and T cells in metastatic lungs and effectively treat low-burden metastases

Shih-Wen Huang[1,2,#], Yein-Gei Lai[1,#], Hao-Ting Liao[1,3,#], Chin-Ling Chang[1], Ruo-Yu Ma[1], Yung-Hsiang Chen[1], Yae-Huei Liou[1], Zhen-Qi Wu[1], Yu-Chen Wu[4], Ko-Jiunn Liu[4], Yen-Tsung Huang[5], Jen-Lung Yang[1], Ming-Shen Dai[6*], and Nan-Shih Liao[1,2*]

[1]Institute of Molecular Biology, Academia Sinica, Taipei, Taiwan

[2]Molecular and Cell Biology, Taiwan International Graduate Program, Academia Sinica and Graduate Institute of Life Science, National Defense Medical Center, Taipei, Taiwan

[3]Department of Life Sciences, National Central University, Taoyuan, Taiwan

[4]National Institute of Cancer Research, National Health Research Institutes, Miaoli, Taiwan

[5]Institute of Statistical Science, Academia Sinica, Taipei, Taiwan

[6]Department of Hematology-Oncology, Tri-Service General Hospital, Taipei, Taiwan

[#]Co-first authors, *Co-corresponding authors

ABSTRACT

Natural killer (NK) cells can control metastasis through cytotoxicity and IFN-γ production independently of T cells in experimental metastasis mouse models. The inverse correlation between NK activity and metastasis incidence supports a critical role for NK cells in human metastatic surveillance. However, autologous NK cell therapy has shown limited benefit in treating patients with metastatic solid tumors. Using a spontaneous metastasis mouse model of MHC-I$^+$ breast cancer, we found that transfer of IL-15/IL-12-conditioned syngeneic NK cells after primary tumor resection promoted long-term survival of mice with low metastatic burden and induced a tumor-specific protective T cell response that is essential for the therapeutic effect. Furthermore, NK cell transfer augments activation of conventional dendritic cells (cDCs), Foxp3$^-$CD4$^+$ T cells and stem cell-like CD8$^+$ T cells in metastatic lungs, which requires IFN-γ of the transferred NK cells. These results imply direct interactions between transferred NK cells and endogenous cDCs to enhance T cell activation. We conducted an investigator-initiated clinical trial of autologous NK cell therapy in six patients with advanced cancer and observed that the NK cell therapy was safe and showed signs of effectiveness. These findings indicate that autologous NK cell therapy is effective in treating established low burden metastases of MHC-I$^+$ tumor cells by activating the cDC-T cell axis at metastatic sites.

34 **Introduction**

35

36 Metastasis is the most common cause of cancer death, and effective therapies for established
37 metastases are currently lacking (Ganesh & Massague, 2021). Natural killer (NK) cells play a
38 critical role in metastasis control, as the abundance of functional circulating or tumor-
39 infiltrating NK cells is inversely correlated with metastasis incidence while being positively
40 correlated with favorable prognoses for patients with or at risk of metastasis (Lopez-Soto,
41 Gonzalez, Smyth, & Galluzzi, 2017). NK cells are capable of recognizing tumor cells via
42 various activating and inhibitory NK receptors (NKRs). Tumor cells often down-regulate the
43 expression of ligands for inhibitory NKRs, yet express stress-induced ligands for activating
44 NKRs. Upon encountering tumor cells, the reduced inhibitory NKR engagement and enhanced
45 activating NKR engagement facilitate NK cell activation (Jamieson et al., 2002; Karre,
46 Ljunggren, Piontek, & Kiessling, 2005). NK cells also express receptors for activating
47 cytokines, such as IL-15, IL-12, IL-18 and IL-21, as well as receptors for suppressive factors
48 such as TGF-β and prostaglandin E2 present in the tumor microenvironment (Huntington,
49 Cursons, & Rautela, 2020). The sum of signals transduced through the activating and inhibitory
50 receptors determines NK cell activation. Activated NK cells kill engaged tumor cells via
51 perforin, granzymes, and the death receptor ligands TNF-α, TRAIL and FasL (Smyth et al.,
52 2005). Activated NK cells also produce IFN-γ, which directly inhibits tumor cell growth and
53 induces type 1 T helper cell (T_H1) and cytotoxic $CD8^+$ T cell responses that are critical for
54 effective anti-tumor immunity (Alspach, Lussier, & Schreiber, 2019; Martin-Fontecha et al.,
55 2004). Moreover, intratumoral NK cells produce XCL1 and CCL5 to recruit type 1
56 conventional dendritic cells (cDC1) that cross-present cell-associated tumor antigen to $CD8^+$
57 T cells (Bottcher et al., 2018), and also produce Flt3L to increase the abundance of cDCs (Barry
58 et al., 2018). However, the immunosuppressive microenvironment induced by tumor cells

59 elicits NK cell and T cell dysfunction (Melaiu, Lucarini, Cifaldi, & Fruci, 2019; Thommen &
60 Schumacher, 2018).
61
62 Two anti-metastatic mechanisms of NK cells have been revealed to date, i.e., cytotoxicity and
63 IFN-γ production. In the metastatic cascade, the epithelial-mesenchymal transition increases
64 the susceptibility of tumor cells to NK cell cytotoxicity by modulating the expression of ligands
65 for the activating NKRs NKG2D (Lopez-Soto et al., 2013), E-cadherin and cell adhesion
66 molecule 1 (Chockley et al., 2018), as well as MHC class I (MHC-I) molecules (Chen et al.,
67 2015). The IFN-γ produced by NK cells was shown to be essential for natural resistance to lung
68 metastasis in a B16 melanoma model (Takeda et al., 2011) and for the IL-12-mediated
69 suppression of liver metastasis in a CT-26 model (Uemura et al., 2010) using *Rag* knockout
70 mice that lacked T cells. Another study indicated that the anti-metastasis effect of IL-12
71 produced by Baft3-dependent DCs is mediated through IFN-γ production by NK cells without
72 the involvement of T cells (Mittal et al., 2017). NK cells also sustain the dormancy of metastatic
73 tumor cells seeded in distal organs through cytotoxicity and IFN-γ (Correia et al., 2021;
74 Malladi et al., 2016). The anti-metastatic mechanisms described above do not involve T cells.
75 Thus, whether T cell immunity plays a role in the anti-metastatic function of NK cells remains
76 to be elucidated.
77
78 Despite the clear anti-tumor function of endogenous NK cells, adoptive transfer of ex vivo-
79 expanded autologous NK cells has shown limited clinical benefit in treating patients with
80 metastatic or locally advanced solid tumors, including melanoma, renal cell carcinoma, and
81 digestive cancer (Parkhurst, Riley, Dudley, & Rosenberg, 2011; Sakamoto et al., 2015). Both
82 the immunosuppressive microenvironment induced by tumor cells (Melaiu et al., 2019) and
83 heterogeneity of NK cell subpopulations and their respective functions (Freud, Mundy-Bosse,

84 Yu, & Caligiuri, 2017) likely contribute to this therapeutic limitation. Given the vast array of
85 approaches used for ex vivo expansion of NK cells (Fang, Xiao, & Tian, 2017), different
86 methods may result in NK cells exerting different functions. We hypothesize that autologous
87 NK cells with anti-tumor activities are effective in treating low burden metastases. In this study,
88 we used syngeneic IL-15/IL-12-conditioned NK cells to treat established lung metastases after
89 resection of the primary MHC-I$^+$ EO771 mammary tumor. We found that the NK cell therapy
90 promoted long-term survival of mice with low metastatic burden in a CD8$^+$ T cell-dependent
91 manner, and induced tumor-specific protective immune memory. Furthermore, NK cell
92 transfer augmented the activation of cDC1, cDC2 and T cells in metastatic lungs, which
93 requires IFN-γ of the transferred NK cells. We also conducted an investigator-driven clinical
94 trial of autologous NK cell therapy on six patients hosting four cancer types and found that the
95 therapy is safe and shows signs of efficacy.
96
97
98 **Results**
99
100 **Characterization of ex vivo-expanded murine NK cells**
101 To generate NK cells with anti-tumor activity ex vivo, we cultured murine BM cells with IL-
102 15 and IL-12, since IL-15 is an NK cell growth and survival factor and both cytokines enhance
103 IFN-γ production and the cytotoxicity of NK cells (Kennedy et al., 2000; Lodolce et al., 1998;
104 Marcenaro et al., 2005). On average, 86% of the resulting cells were identified as TCRαβ$^-$
105 TCRγδ$^-$CD19$^-$NK1.1$^+$ that express NKG2D, EOMES and T-bet (Figure 1A), representing
106 characteristics of NK cells (Gordon et al., 2012; Raulet, 2003). Approximately 90% of the
107 expanded NK cells were CD27$^+$ with no-to-low levels of CD11b expression (Figure 1A). The
108 proportion of NK cells expressing MHC-I-interacting NKRs, including activating Ly49D/H

109 and inhibitory Ly49A/G2/I and NKG2A, was stable among independent cultures (Figure 1B).
110 In terms of activation status, on average, 87% of the expanded NK cells expressed either
111 intermediate or high levels of the activating receptor DNAM-1 and 82% of them displayed an
112 activated $B220^{+}CD11c^{+}$ phenotype (Figure 1C). Consistently, they expressed the anti-tumor
113 effectors IFN-γ, granzyme B, and TRAIL (Figure 1D). Co-culturing the NK cells with either
114 EO771 breast adenocarcinoma cells that express MHC-I molecules and Rae-1 or B16F10
115 melanoma cells that express none of those molecules in vitro (Figure 1-figure supplement 1)
116 resulted in dose-dependent tumor cell death (Figure 1E) and up-regulation of IFN-γ production
117 by the NK cells (Figure 1F). Thus, the NK cells conditioned by means of IL-15 and IL-12
118 possess anti-tumor activities in vitro.

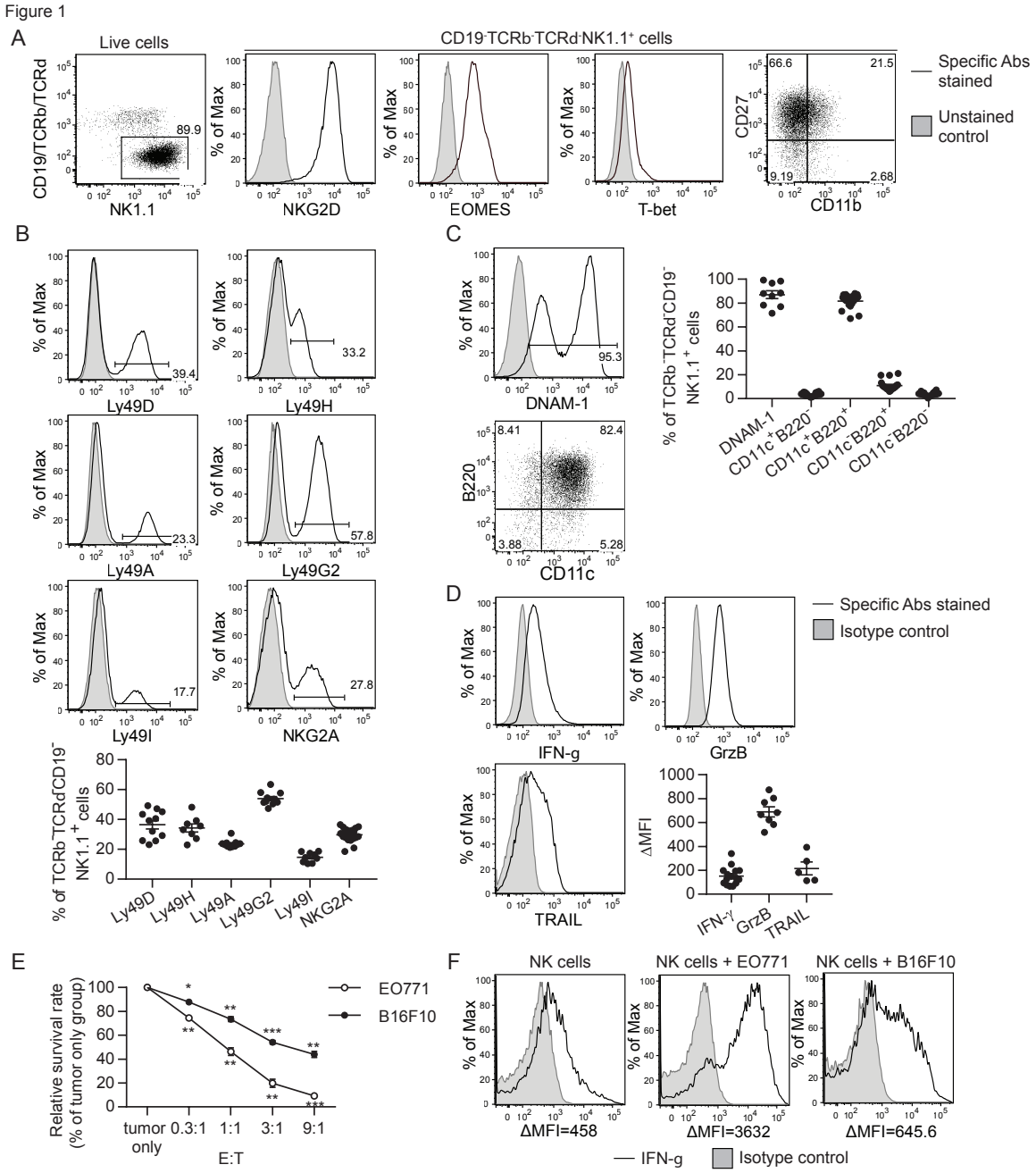

Figure 1. Characterization of ex vivo-expanded murine NK cells.

BM cells were cultured with IL-15 and IL-12 as described in Methods. (A) Analysis of NK cells ($CD19^-TCR\alpha\beta^-TCR\gamma\delta^-NK1.1^+$) among live expanded cells. Plots are representative of 20 independent cultures. (B)-(D) Expression of MHC-I-interacting activating and inhibitory NKRs, activation markers and anti-tumor effectors by the expanded NK cells. Representative flow histograms are presented for each molecule, and the compiled data from independent expansion cultures is indicated by the dot plots. (E) In vitro cytotoxicity of the expanded NK cells. CFSE-labeled EO771 or B16F10 cells (T, target) were co-cultured with expanded NK cells (E, effector) at the indicated E:T ratios. Tumor cell viability was analyzed by PI staining using FACS. One representative of three independent experiments is shown. Data represent mean ± SEM of triplicate wells. Statistical significance was determined by unpaired two-tailed Student's t-test: $*P<0.05$, $**P<0.01$, $***P<0.001$ relative to tumor only. (F)

131 Tumor cells stimulate IFN-γ production by the expanded NK cells. Sorted NK cells were cultured alone (NK cells)
132 or together with tumor cells (NK cells + EO771 and NK cells + B16F10) at a ratio of 1:1. Levels of intracellular
133 IFN-γ of NK cells were determined by staining with anti-IFN-γ or isotype control antibody, and analyzed by
134 FACS. The difference in mean fluorescence intensity (ΔMFI) was calculated by subtracting the MFI value of
135 isotype control staining from that of anti-IFN-γ antibody staining. Representative plots of two independent
136 experiments are shown.
137 **Figure supplement 1.** Expression of MHC-I molecules and Rae-1 by EO771 and B16F10 cells *in vitro*.

138 **EO771 tumor-resected mice represent a model for established metastases to test NK cell**
139 **therapy**

140 Cancer recurrence occurs in a significant proportion of patients after primary tumor resection
141 due to dissemination of tumor cells before and/or during surgery. To mimic that scenario, we
142 established a syngeneic orthotopic breast cancer model using the MHC-I$^+$ EO771 cell line that
143 harbors numerous mutations (Y. Yang et al., 2017). At 21 days post-inoculation and consistent
144 with the spontaneous lung metastatic property of the EO771 line (Ewens, Mihich, & Ehrke,
145 2005), we observed that ~85% of mice with a primary tumor weighing ≥ 95 mg had metastatic
146 foci on the lung surface. The number and area of metastatic foci was positively correlated with
147 tumor weight on day 21 (Figure 2A). Resection of the primary tumor and its sentinel lymph
148 node (LN) on day 21 resulted in a long-term survival rate of 18%, with mortality of all
149 remaining mice (Figure 2B). All dead mice exhibited metastases in the lung, of which 71%
150 displayed tumor reappearance at the surgical site (data not shown). Therefore, this tumor
151 resection model represents a model of established metastases caused by tumor cell
152 dissemination before and arising from surgery. To apply adoptive NK cell therapy to this model,
153 we examined if the transferred NK cells reach the lungs of tumor-resected mice. The expanded
154 NK cells express the chemokine receptors CXCR3, CCR5 and CXCR6 (Figure 2C), and the
155 lung of tumor-resected mice express mRNA of the corresponding ligands CXCL9/10/11,
156 CCL3/4/5 and CXCL16 (Figure 2D). Using eGFP$^+$ NK cells, we observed that numbers of
157 transferred cells in the lung peaked at 4 h and then continuously declined, remaining detectable
158 for at least 2 days (Figure 2E). A similar pattern of transferred NK cells was observed in the
159 spleen, albeit with lower cell counts (Figure 2E).

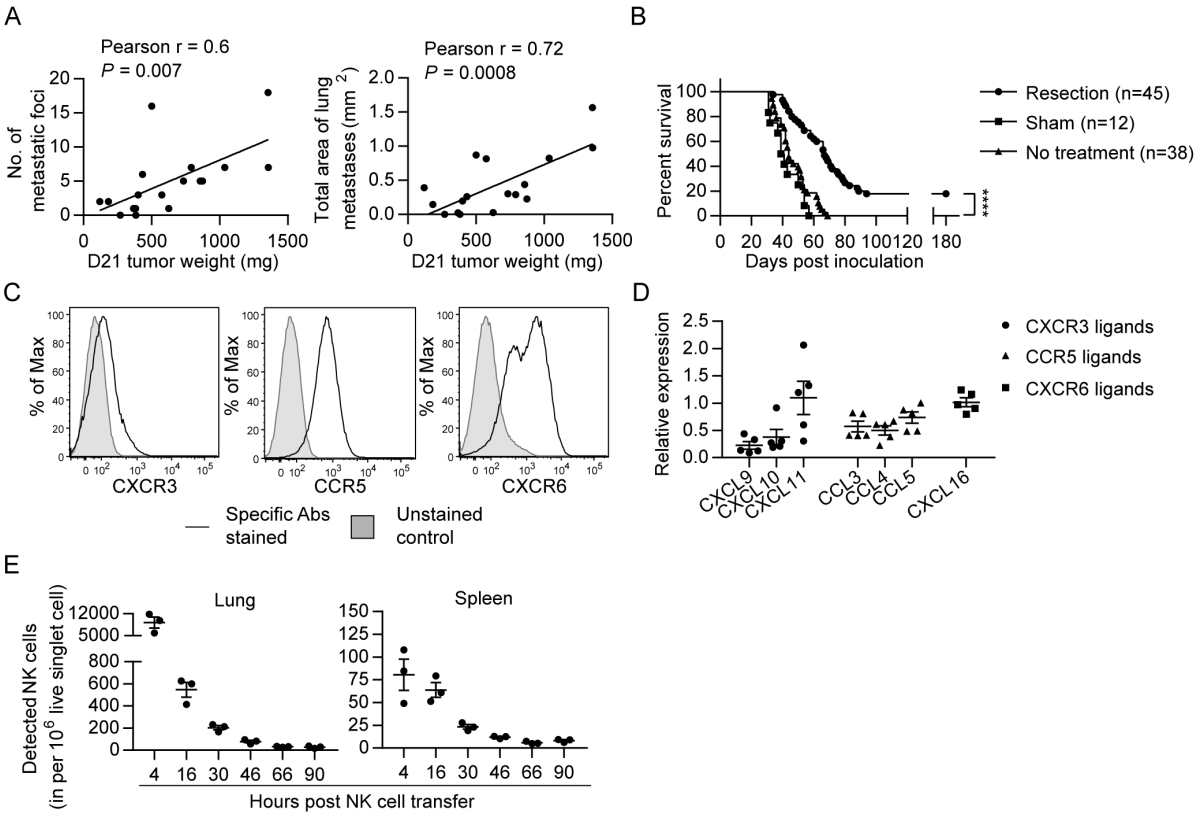

Figure 2. EO771 tumor resection and metastasis model for NK cell treatment**.**

(A) Positive correlation between primary tumor weight and lung metastasis. Pearson correlations between day 21 tumor weights and the number and total area of metastatic foci on the lung surface are shown. Each dot represents a mouse. (B) Survival of mice who received day 21 tumor resection, sham surgery, or no treatment. Mouse survival was analyzed by means of the Kaplan-Meier estimator and a Log-Rank test: ****P<0.0001. (C) Expanded NK cells express the chemokine receptors CXCR3, CCR5 and CXCR6. Representative flow plots of 10 independent cultures are shown. (D) Expression of CXCR3, CCR5 and CXCR6 ligands in the lung. Specific gene expression was determined by quantitative real-time PCR using lung RNA of day 21 tumor-resected mice collected on day 24 post tumor inoculation and normalized to the expression of cyclophilin a. Each symbol represents a mouse and means ± SEM are shown. (E) Expanded eGFP^{+} NK cells were transferred into day 21 EO771-resected mice on day 24, and quantified in the single cell suspensions of spleen and lung at the indicated times using FACS. Numbers of eGFP^{+} NK cells detected in each organ are shown. Each dot represents a mouse (means ± SEM).

175 **Syngeneic NK cell therapy is effective in treating mice with low metastatic burden in a**
176 **$CD8^+$-T-cell-dependent manner**
177 We evaluated the effect of syngeneic NK cell therapy on tumor-resected mice (Figure 3A
178 Schema), and found a negative correlation between survival time and day 21 tumor weight in
179 the NK cell-treated group but not in the control group (Figure 3A). Consequently, we divided
180 the mice into two groups according to their day 21 tumor weight. NK cell-treated mice
181 displayed significantly enhanced overall survival (OS) and an improved long-term survival rate
182 from 33% to 68% compared to control mice in the 95-400 mg tumor group, whereas the same
183 therapy did not improve OS of the > 400 mg tumor group (Figure 3B). These results, together
184 with the result presented in Figure 2A, indicate that the NK cell therapy promotes long-term
185 survival of tumor-resected mice carrying low metastatic burden. We further examined if the
186 surviving mice after NK cell treatment had acquired tumor-specific protection by re-
187 challenging them with either EO771 or B16F10 tumor cells (Figure 3C Schema). We found
188 that 83% of these mice were protected from EO771 re-challenge and survived beyond 180 days,
189 whereas all mice re-challenged with B16F10 died (Figure 3C). Age-matched naïve mice
190 inoculated for the first time with either EO771 or B16F10 as a control all died (Figure 3C).
191 Thus, surviving mice of post-resection NK cell therapy displayed tumor-specific protective
192 immunity.
193
194 Since the tumor re-challenge experiment was performed at 11-13 weeks following NK cell
195 treatment (Figure 3C), the observed long-lasting protection is likely mediated by memory T
196 cells. Accordingly, we examined the role of T cells in NK cell therapy by depleting T cell
197 subsets two days before resecting the primary tumor (Figure 3D Schema and Figure 3-figure
198 supplement 1). Treatment with anti-CD8 antibody alone or with anti-CD4 plus anti-CD8
199 antibodies, but not with anti-CD4 antibody alone, abolished the therapeutic effect of NK cell

200 therapy (Figure 3D), indicating the essential role of $CD8^+$ T cells. Moreover, mice depleted of
201 $CD8^+$ cells alone survived better than mice depleted of both $CD4^+$ and $CD8^+$ cells in response
202 to NK cell therapy (Figure 3D), suggesting a $CD8^+$-T-cell-independent anti-tumor effect of
203 $CD4^+$ T cells. Next, we examined whether the T cells in surviving mice after NK cell therapy
204 and tumor re-challenge possess anti-tumor activity. T cells and non-T cells were isolated from
205 individual NK cell-treated and EO771-rechallenged survivors or from age-matched donors,
206 and then transferred into naïve recipients in a 1-donor-to-1-recipient manner. The recipient
207 mice were inoculated with EO771 cells to evaluate the anti-tumor effects of the donor cells,
208 whereas naïve mice received no donor cells and served as a control for tumor growth (Figure
209 3E Schema). For the mice receiving cells isolated from the survivors, 5 of 6 T-cell recipients
210 and 1 of 6 non-T-cell recipients survived beyond 120 days post tumor inoculation (Figure 3E).
211 In contrast, mice receiving either T or non-T cells isolated from age-matched naïve donors all
212 died. Mice that received no donor cells in both experiments also all died (Figure 3E). Together,
213 these results indicate that the post-resection NK cell therapy induces a tumor-specific T cell
214 response with memory that is essential for its treatment efficacy.

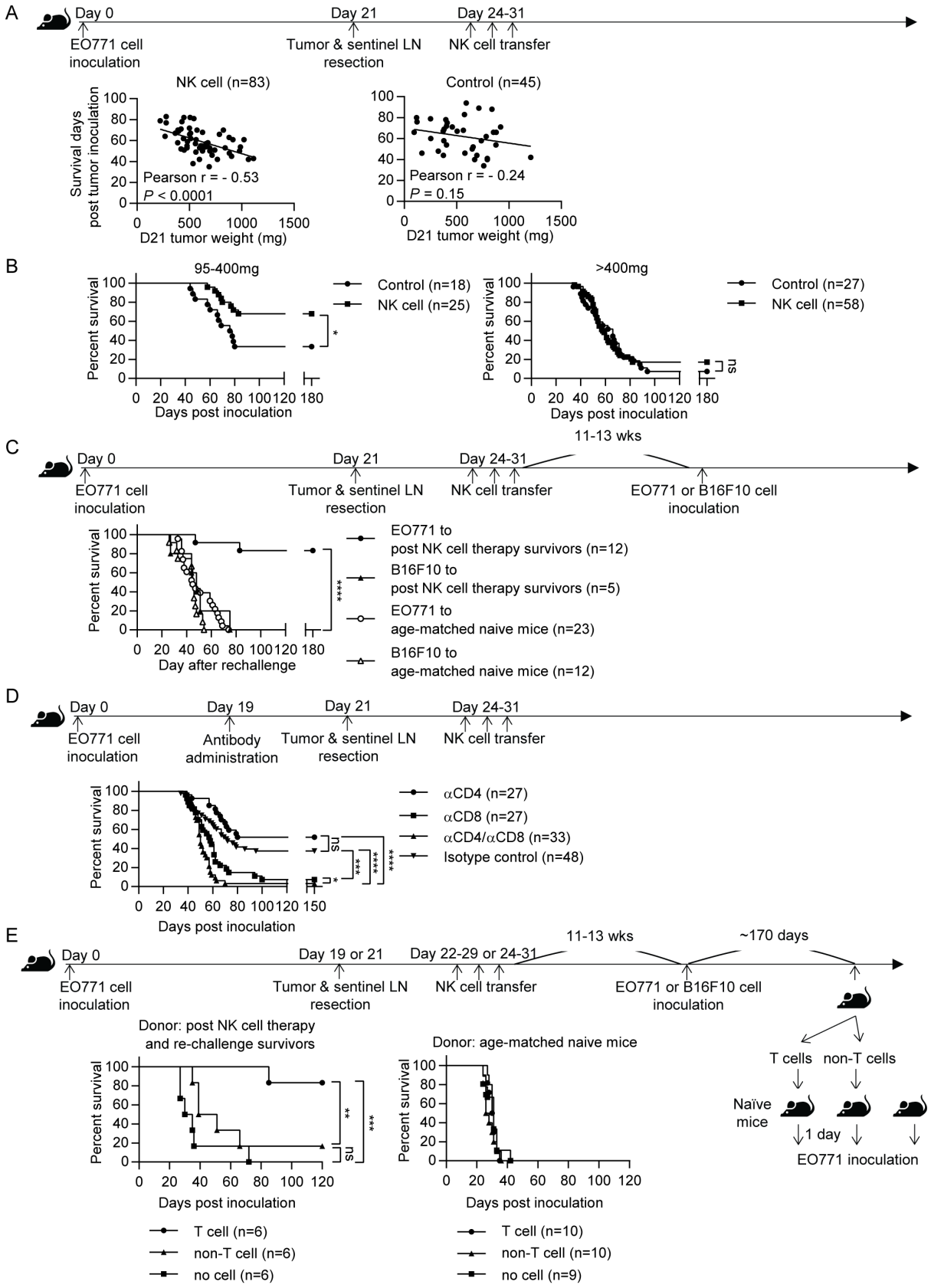

Figure 3. Syngeneic NK cell therapy is effective in treating mice with low metastatic burden in a CD8^{+}-T-cell-dependent manner.

219 (A) Day 21 tumor weight is inversely correlated with survival duration of NK-cell-treated tumor-resected mice.
220 After tumor and sentinel LN resection on day 21, mice received either sorted NK cells (NK cell) or PBS (Control)
221 at the indicated time-points. The correlation between day 21 tumor weight and survival time of mice was evaluated
222 by Pearson correlation. Each dot represents a mouse. The results have been compiled from 5-8 independent
223 experiments. The Control group is the same dataset as presented for the Resection group in Figure 2B. (B) NK
224 cell therapy promotes long-term survival of mice who had light tumors on day 21. The mice described in (A) were
225 separated into 95-400 mg and >400 mg day 21 tumor weight groups for survival analysis by means of the Kaplan-
226 Meier estimator and a Log-Rank test: *P<0.05. (C) NK cell therapy induces tumor-specific protection. Surviving
227 mice after NK cell therapy were rechallenged with EO771 (●, compiled from four independent experiments) or
228 B16F10 cells (▲, compiled from two independent experiments) at 11-13 weeks post therapy, and then monitored
229 for survival. Age-matched naïve mice were inoculated with EO771 (○, compiled from four independent
230 experiments) or B16F10 cells (△, compiled from three independent experiments) as controls. Mouse survival,
231 using 2000 mm^3 tumor volume as a cut-off, was analyzed by means of the Kaplan-Meier estimator and a Log-
232 Rank test: ****P<0.001. (D) Depletion of $CD8^+$ cells abolished the efficacy of NK cell therapy. Mice were treated
233 with indicated antibodies at day 19 post tumor inoculation, and then received resection followed by NK cell
234 therapy. Mouse survival was analyzed by means of the Kaplan-Meier estimator and a Log-Rank test: ns, not
235 significant; *P<0.05; ***P<0.001; ****P<0.0001. The data are compiled from 2-3 experiments. (E) T cells
236 isolated from surviving mice post NK cell therapy and tumor re-challenge confer anti-tumor activity. Post NK
237 cell therapy and re-challenge survivors were collected from three independent experiments. T cells and non-T
238 cells isolated from each survivor were transferred separately into naïve recipient mice in a 1-donor-to-1-recipient
239 manner, whereas other naïve mice that received no cells served as a control (compiled from two independent
240 experiments). T cells and non-T cells were also isolated from age-matched naïve donors and transferred separately
241 into naïve recipient mice, whereas other naïve mice that received no cells served as a control (compiled from two
242 independent experiments). The recipient mice were then inoculated with EO771 cells one day after cell transfer.
243 Mouse survival, using 2000 mm^3 tumor volume as a cut-off, was analyzed by means of the Kaplan-Meier
244 estimator and a Log-rank test: ns, not significant; **P<0.01; ***P<0.001.
245 **Figure supplement 1.** Effectiveness of in vivo depletion of $CD4^+$ and $CD8^+$ T cells by antibody (related to Figure
246 3D).

247 **Syngeneic NK cell transfer promotes cDC and T cell activation in metastatic lungs**

248 Conventional DCs directly trigger an antigen-specific T cell response by providing ligands to
249 antigen, costimulatory and cytokine receptors expressed on T cells (Cabeza-Cabrerizo,
250 Cardoso, Minutti, Pereira da Costa, & Reis e Sousa, 2021). A previous in vivo study reported
251 that A20 lymphoma expressing abnormally low levels of MHC I molecules (MHC-I) induces
252 IL-12 production by splenic DCs ($CD11c^{+}CD19^{-}F4/80^{-}$) and $CD8^{+}$ T cell response (Mocikat et
253 al., 2003). Therefore, we hypothesized that our NK cell therapy would modulate cDCs in
254 metastatic lungs in favor of a T cell response. As our IL-15/IL-12-conditioned NK cells express
255 high levels of mRNA encoding IFN-γ and IL-10 (data not shown), cytokines known to
256 modulate cDC function, we examined whether one transfer of wild type (WT), *Il10*$^{-/-}$ or *Ifng*$^{-/-}$
257 NK cells affected cDCs and T cells in the metastatic lungs. Immune cells were analyzed ~18
258 hours after NK-cell transfer, by which time the level of transferred NK cells in the lung declined
259 by > 60% relative to that determined at 4-hours (Fig. 2E).

260

261 We found that lung cDC1s and cDC2s consist of cells expressing either high or low level of
262 MHC-II (MHC-II^{hi} or MHC-II^{lo}), and the MHC-II^{hi} cDCs are composed of $CCR7^{+}Lamp3^{+}$ and
263 $CCR7^{-}Lamp3^{-}$ subsets (Figure 4A). The $CCR7^{+}Lamp3^{+}$MHC-II^{hi} subset expresses the highest
264 level of APC function molecules, including MHC-I, MHC-II, CCR7, CD86, CD40 and PD-L1
265 (Figure 4A), resembling the recently identified mregDC (Cheng et al., 2021; de Saint-Vis et
266 al., 1998; Maier et al., 2020). The $CCR7^{-}Lamp3^{-}$MHC-II^{hi} subset expresses an intermediate
267 level of MHC-II, CD86 and CD40 among the three subsets, and similar levels of MHC-I, CCR7
268 and PD-L1 to that of the MHC-II^{lo} subset (Figure 4A). NK-cell transfer did not alter the
269 proportion of total cDC1s or cDC2s in $CD45^{+}$ cells in the lung tissue (data not show). However,
270 among cDC1s, transfer of WT NK cells significantly increased the proportion of the MHC-II^{hi}
271 subsets, the levels of CD86 and CD40 expressed by all three subsets, and the levels of PD-L1,

272 MHC-I and MHC-II expressed by the CCR7^{-}Lamp3^{-}MHC-II^{hi} and MHC-II^{lo} subsets (Figure
273 4B). These effects require IFN-γ, but not IL-10, of the transferred NK cells, except for the PD-
274 L1 level in the MHC-II^{lo} subset (Figure 4B). Transfer of WT NK cells exerted many effects on
275 cDC2s similar to those described above for cDC1s, albeit with several differences (Figure 4B).
276 The differences include augmenting the MHC-II level in the CCR7^{+}Lamp3^{+}MHC-II^{hi} subset,
277 reducing the MHC-II level in the MHC^{lo} subset, and having no effect on the level of CD40 in
278 the CCR7^{+}Lamp3^{+}MHC-II^{hi} subset (Figure 4B). IFN-γ of transferred NK cells is essential for
279 all effects on cDC2s except for the increase of the CCR7^{+}Lamp3^{+}MHC-II^{hi} subset, the
280 increased levels of CD40 and MHC-II in the CCR7^{-}Lamp3^{-}MHC-II^{hi} subset, and the increased
281 levels of CD86 and MHC-II in the MHC-II^{lo} subset (Figure 4B).

A

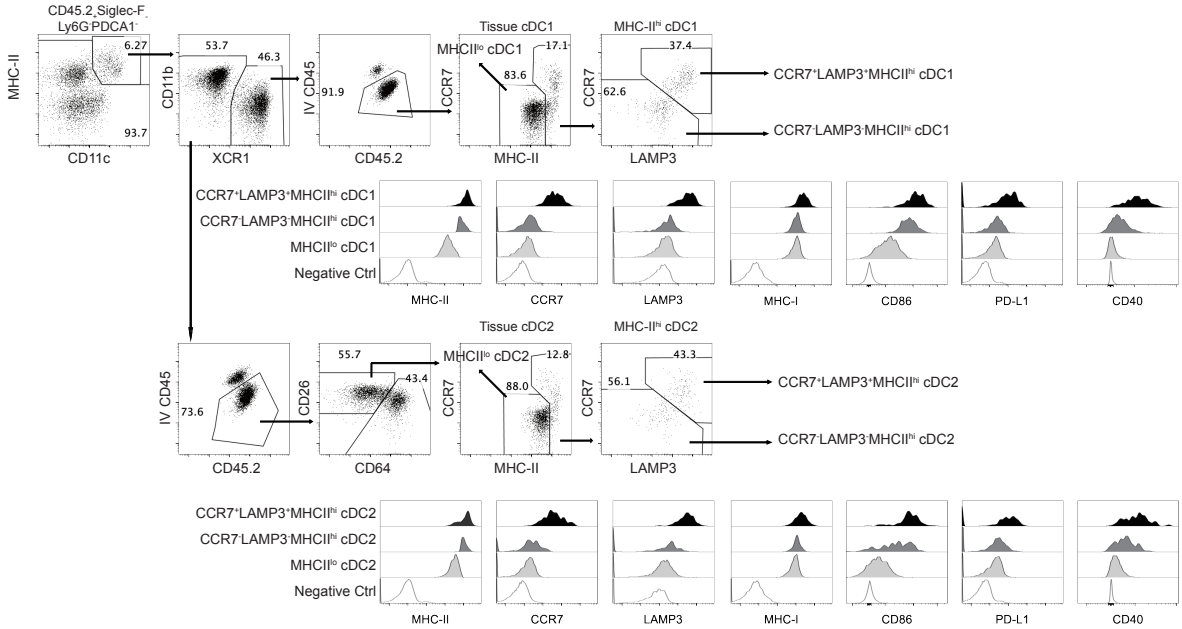
CD45.2⁻Siglec-F⁻
Ly6G⁻PDCA1⁻
MHC-II
CD11c
6.27
93.7
CD11b
XCR1
53.7
46.3
IV CD45
CD45.2
91.9
Tissue cDC1
MHCIIlo cDC1
CCR7
MHC-II
17.1
83.6
MHC-IIhi cDC1
CCR7
LAMP3
37.4
62.6
CCR7+LAMP3+MHCIIhi cDC1
CCR7-LAMP3-MHCIIhi cDC1
CCR7+LAMP3+MHCIIhi cDC1
CCR7-LAMP3-MHCIIhi cDC1
MHCIIlo cDC1
Negative Ctrl
MHC-II
CCR7
LAMP3
MHC-I
CD86
PD-L1
CD40
IV CD45
CD45.2
73.6
CD26
CD64
55.7
43.4
Tissue cDC2
MHCIIlo cDC2
CCR7
MHC-II
12.8
88.0
MHC-IIhi cDC2
CCR7
LAMP3
43.3
56.1
CCR7+LAMP3+MHCIIhi cDC2
CCR7-LAMP3-MHCIIhi cDC2
CCR7+LAMP3+MHCIIhi cDC2
CCR7-LAMP3-MHCIIhi cDC2
MHCIIlo cDC2
Negative Ctrl
MHC-II
CCR7
LAMP3
MHC-I
CD86
PD-L1
CD40

282

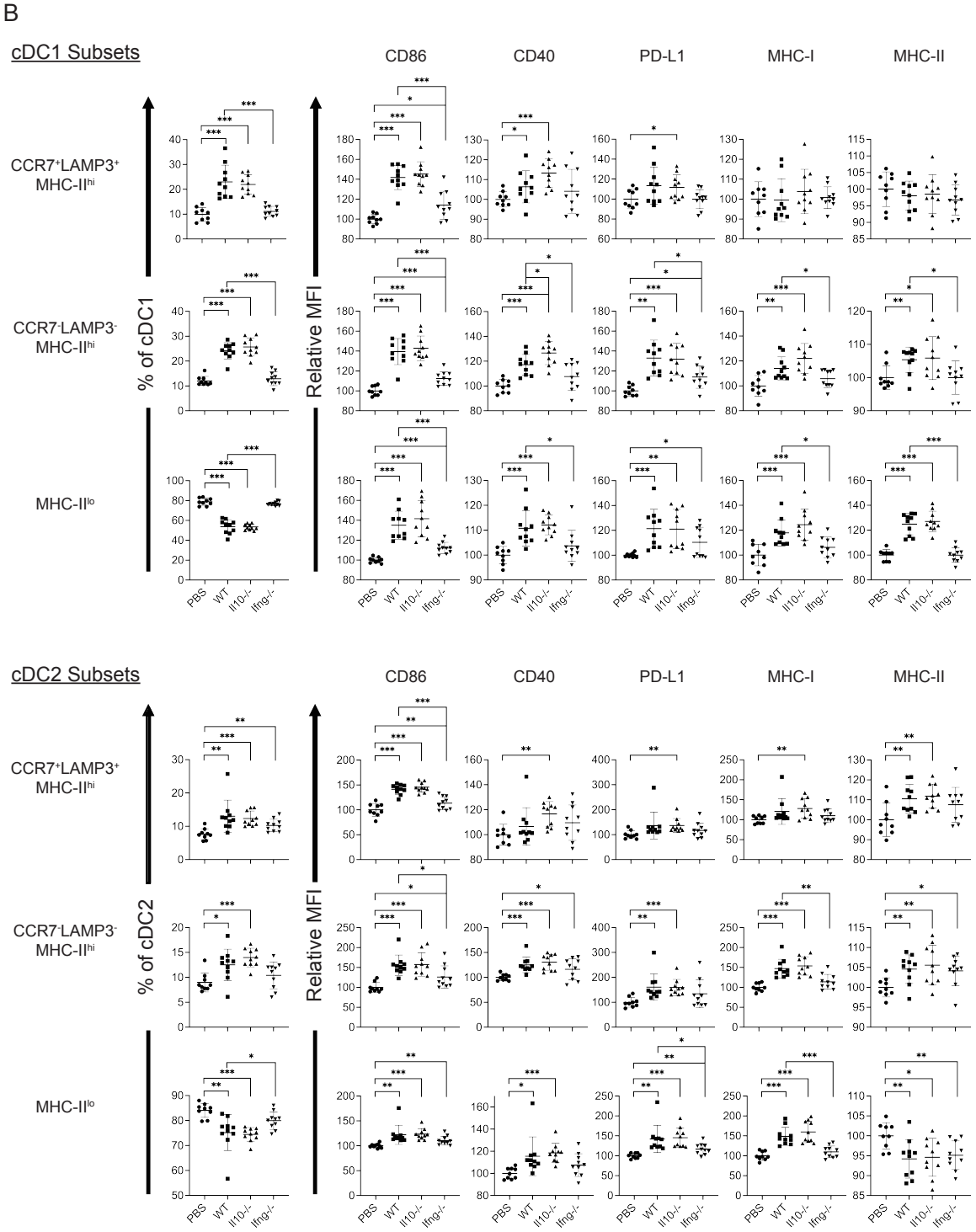

Figure 4. Syngeneic NK cell transfer modulates APC function of cDC in the metastatic lungs. The experimental design is the same as depicted in the Fig. 3A schema except that NK cells (WT, *Il10*$^{-/-}$ or *Ifng*$^{-/-}$) were transferred once on day 24 and lung immune cells were analyzed on day 25. (A) Gating strategies and characterization of cDC subsets in lung tissue. The dot plots show the gating of CCR7^{+}LAMP3^{+}MHC-II^{hi}, CCR7^{-}LAMP3^{-}MHC-II^{hi} and MHC-II^{lo} subsets of cDC1s and cDC2s. The histograms show the comparison of indicated molecules expressed by the three subsets of cDC1s and cDC2s. Negative controls are either fluorescence-minus-one (FMO) or single stain of another molecule. Data shown are from a representative PBS-treated mouse. (B)

292 NK-cell transfer affects the activation of lung cDCs. The proportion of the three cDC subsets in cDC1s and cDC2s
293 are shown. The expression of the indicated APC function molecules was analyzed as relative MFI, based on
294 normalization against the mean MFI of the PBS group in each independent experiment. Data are compiled from
295 two independent experiments and presented as mean ± SEM. Each symbol represents one mouse. Statistical
296 significance was determined by unpaired two-tailed Student's t-test: *P≤0.05, **P≤0.01, ***P≤0.001.

297 Next, we examined T cells in the lung tissue. Transfer of WT NK cells increased the proportion
298 of Foxp3$^-$CD4$^+$ and CD8$^+$ T cells without altering that of Foxp3$^+$CD4$^+$ T cells (Figure 5A and
299 Figure 5-figure supplement 1A). The proportion of activated Foxp3$^-$CD4$^+$ T cells, including
300 effector (CD62L$^-$CD44$^+$), PD-1$^+$ and Ki67$^+$ subsets, also increased (Figure 5B and Figure 5-
301 figure supplement 1A). These effects were not observed for mice that received *Ifng*$^{-/-}$ NK cells
302 (Figure 5B). CD8$^+$ T cells in a tumor microenvironment (TME) are known to display a complex
303 composition comprising subsets of different activation/differentiation statuses. First, we
304 categorized lung tissue CD8$^+$ T cells according to PD-1 and Lag3 expression (Figure 5-figure
305 supplement 1A), because PD-1 expression is induced by TCR stimulation (Sharpe & Pauken,
306 2018) and Lag3 is only expressed by exhausted or progenitor-exhausted (PEX) CD8$^+$ T cells
307 (Calagua et al., 2021; Z. Z. Yang et al., 2017). We reasoned that PD-1$^-$Lag3$^-$ CD8$^+$ T cells
308 (Figure 5-figure supplement 1A) are either naïve or at a very early stage of activation, and
309 found that transfer of *Il10*$^{-/-}$, but not WT, NK cells increased the proportion of CD62L$^+$CD44$^+$
310 and CD62L$^-$CD44$^+$ subsets, while the proportion of CD62L$^-$CD44$^+$ and Ki67$^+$ subsets were
311 lower in mice that received *Ifng*$^{-/-}$ NK cells compared to those proportions in mice that received
312 WT NK cells (Figure 5C). These results indicate that IL-10 of transferred NK cells inhibits
313 activation of naïve CD8$^+$ T cells, whereas IFN-γ of transferred NK cells promotes their effector
314 differentiation and proliferation. We further examined stem cell-like (SCL) CD8$^+$ T cells that
315 are Tim3$^-$ in PD-1^{lo}Lag3$^-$ CD8$^+$ cells (Figure 5-figure supplement 1A) (Castiglioni et al., 2023),
316 and detected an increase of total and Ki67$^+$ SCL CD8$^+$ T cells in mice that received WT or *Il10*$^-$
317 $^{/-}$, but not *Ifng*$^{-/-}$, NK cells (Figure 5D). Transfer of *Il10*$^{-/-}$ NK cells resulted in a higher level of
318 SCL CD8$^+$ T cells than when WT NK cells were transferred (Figure 5D). In contrast, NK cell
319 transfer did not alter the proportion of exhausted or PEX CD8$^+$ T cells (Figure 5D and Figure
320 5-figure supplement 1A). The expression of PD-1, Lag3, Tim3, CD44, CD62L, Ly108 and
321 GrzB by SCL, exhausted, and PEX CD8$^+$ T cells in our analysis is consistent with the known

322 characteristics of these cell populations (Figure 5-figure supplement 1B) (Andreatta et al., 2021;
323 Castiglioni et al., 2023; Martinez-Usatorre et al., 2020). Thus, overall, transfer of the IL-15/IL-
324 12-conditioned syngeneic NK cells augmented the activation of cDC1s and cDC2s, as well as
325 the levels and activation of Foxp3^{-}CD4^{+} T cells, naïve CD8^{+} T cells and SCL CD8^{+} T cells in
326 metastatic lungs. Moreover, IFN-γ of the transferred NK cells is essential for these effects.

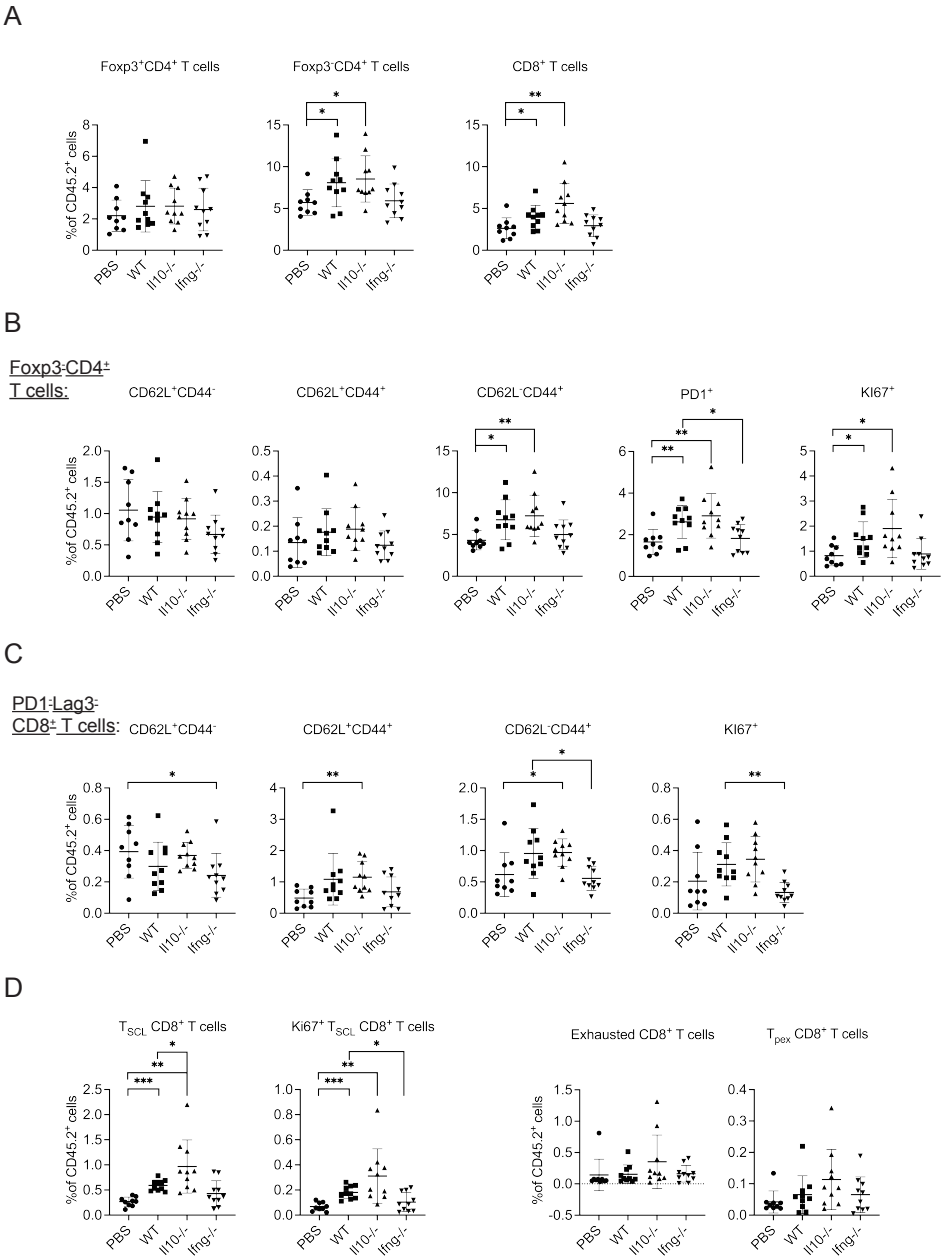

Figure 5. Syngeneic NK cell transfer promotes T cell activation in metastatic lungs.

The experimental design is the same as Figure 4. The proportion of T cell subsets in $CD45^+$ cells in lung tissue were analyzed (Figure 5-figure supplement 1). (A) $Foxp3^+CD4^+$, $Foxp3^-CD4^+$ and $CD8^+$ T cells. (B) $Foxp3^-CD4^+$ T cell subsets. (C) $PD1^-Lag3^-CD8^+$ subsets. (D) Total and $KI67^+$ SCL, exhausted, and PEX $CD8^+$ T cells. Data are compiled from two independent experiments and are presented as mean ± SEM. Each symbol represents one mouse. Statistical significance was determined by unpaired two-tailed Student's t-test: *P≤0.05, **P≤0.01, ***P≤0.001.

Figure supplement 1. Analysis of T cells in lung tissue (related to Figure 5).

337 It is known that CCR7 mediates migration of cDC from tumor to its draining LN (dLN) (Riol-
338 Blanco et al., 2005), in which the migratory cDCs prime tumor-specific naive T cells (Mempel,
339 Henrickson, & von Andrian, 2004). As transfer of WT NK cells increased the levels of
340 $CCR7^{+}LAPM3^{+}MHC\text{-}II^{hi}$ cDC1s and cDC2 in metastatic lungs (Figure 4), we hypothesized
341 that NK cell transfer augments migration of lung cDCs to mLN and activation of T cells. We
342 analyzed migratory and resident cDCs in mLN (Figure 6-figure supplement 1), and found that
343 > 90% of migratory cDC1s and > 65% of migratory cDC2s express CCR7 and LAMP3 (Figure
344 6A), a phenotype similar to lung $CCR7^{+}LAMP3^{+}MHC\text{-}II^{hi}$ cDC1 and cDC2. On the other hand,
345 the great majority of resident cDC1s and cDC2s in mLN are $CCR7^{-}LAMP3^{-}$ (Figure 6A).
346 Transfer of WT NK cells increased the proportion of migratory cDC1 in cDCs and the level of
347 CD86 expression by both migratory cDC1s and cDC2s, which required IFN-γ of the transferred
348 NK cells (Figure 6B). We also examined T cells in mLN and found that NK cell transfer
349 affected neither the proportion nor the activation marked by $CD44^{+}$ or $KI67^{+}$ of $Foxp3^{-}CD4^{+}$
350 and $CD8^{+}$ T cells (data not show). Collectively, NK cell transfer increased the level of
351 migratory cDC1 and CD86 expression by migratory cDC1s and cDC2s, but did not affect T
352 cell activation in mLN.

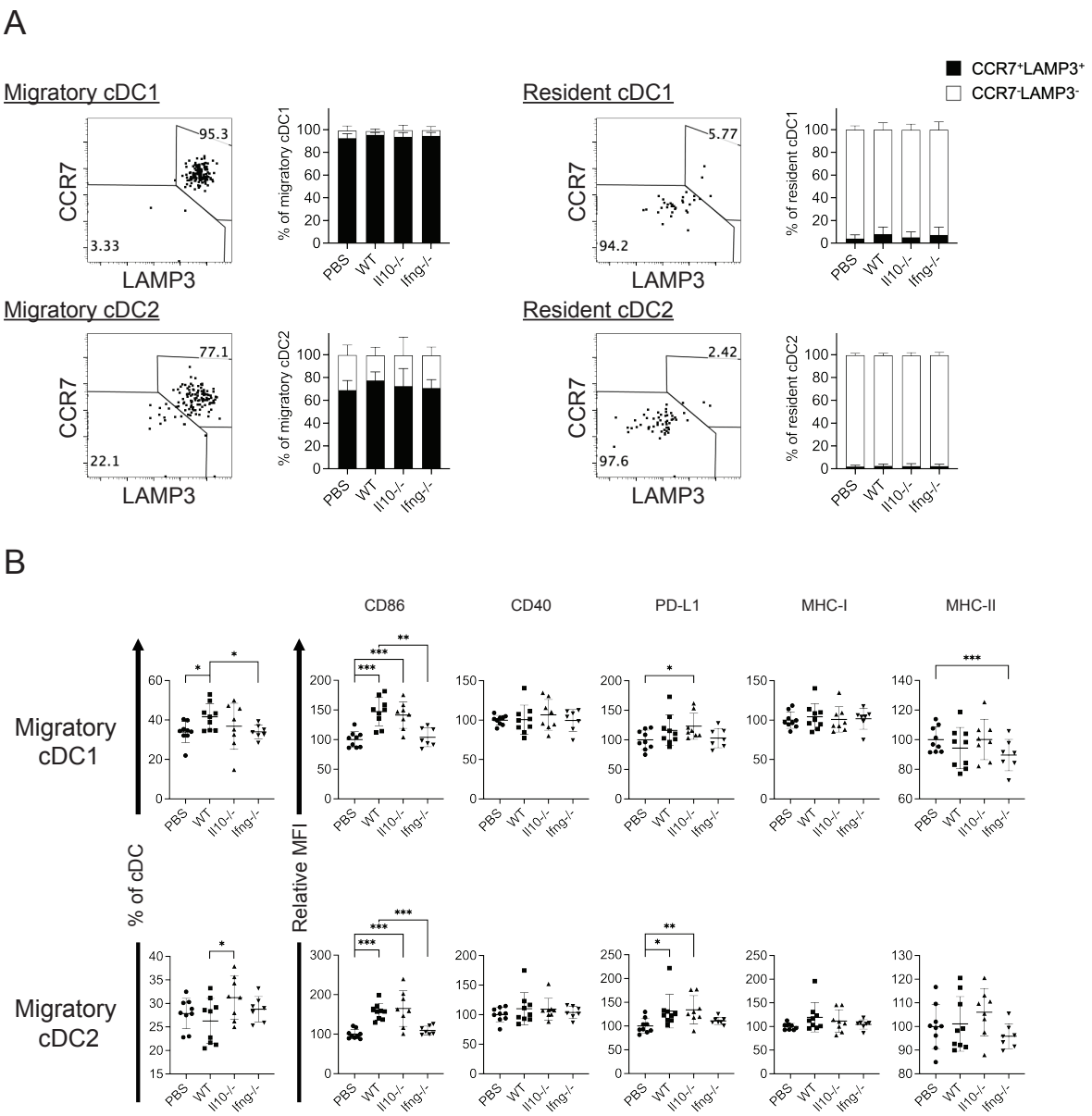

Figure 6. Syngeneic NK cell transfer affects migratory cDCs in mLN.
The experimental design is the same as Fig. 4. (A) The expression of CCR7 and LAMP3 by migratory and resident cDC1s and cDC2s. (B) NK cell transfer affected migratory cDC subsets. The proportion of migratory cDC1s and cDC2s in cDC are shown. The expression of the indicated APC function molecules was analyzed as relative MFI, based on normalization against the mean MFI of the PBS group in each independent experiment. Data are compiled from two independent experiments and presented as mean ± SEM. Each symbol represents one mouse. Statistical significance was determined by unpaired two-tailed Student's t-test: *P≤0.05, **P≤0.01, ***P≤0.001.
Figure supplement 1. Analysis of cDCs in mLN.

363 **Clinical trial of autologous NK cell therapy on advanced cancer patients**

364 To assess NK cell therapy in human, we expanded human NK cells from TCRβ$^-$CD19$^-$ PBMCs.
365 The expanded NK cells are identifiable as CD3$^-$CD19$^-$CD14$^-$CD56$^+$EOMES$^+$, with ~90% of
366 the cells expressing HLA-DR (Figure 7A). Co-culture of the expanded HLA-DR$^+$ NK cells
367 with K562, THP-1 or U937 tumor cells resulted in dose-dependent tumor cell death (Figure
368 7B) and increased IFN-γ production by the NK cells (Figure 7C). We then conducted an
369 investigator-initiated clinical trial of autologous NK cell therapy in six pre-treated advanced
370 cancer patients enrolled between May 2016 and October 2019. Baseline characteristics of these
371 patients are presented in Table. The patients had an ECOG performance status of 0 and a
372 relatively small target lesion size (6.4-22.7 mm), suggesting relatively low tumor burden. The
373 patients in cohort 1 and cohort 2 received six bi-weekly infusions of 20×10^6 or 30×10^6
374 autologous HLA-DR$^+$ NK cells, respectively. The infused cells were total cells expanded from
375 TCRβ$^-$CD19$^-$ PBMCs, of which median 92.4% (83.2-94.9%) were HLA-DR$^+$ NK cells (Figure
376 8A and Figure 8-figure supplement 1). The composition of the infused cells differed slightly
377 among patients, but was stable for each patient over the six infusions (Figure 8A). We
378 examined the expression of NKRs, CD16 and CXCR3 on the HLA-DR$^+$ NK cells and
379 determined that it was stable for each patient over six batches of cell preparations, apart from
380 some variation in NKp44 for patient 5 and CXCR3 for patient 4 (Figure 8B and Figure 8-figure
381 supplement 2). Moreover, the HLA-DR$^+$ NK cells expressed the anti-tumor effectors perforin
382 and IFN-γ (Figure 8C and Figure 8-figure supplement 3). All patients completed the course of
383 six infusions. The therapy proved safe and was well-tolerated by all patients, as no treatment-
384 related adverse effect was observed throughout the entire infusion period up to 24 h after the
385 final infusion. We assessed the preliminary impact of this therapeutic approach based on
386 clinical responses and OS, and present the results with a median follow-up of 60.0 months
387 (2.73-60.0). The response and survival timings were counted from the first infusion of NK cells

388 (Figure 8D). We adopted RECIST 1.1 to evaluate responses, except that the baseline target
389 lesions for patients 3, 4 and 5 (Table) were 18%, 36% and 31% smaller than measurable lesions
390 according to RECIST 1.1. All patients were in a stable disease (SD) state at month 1 (i.e., 1
391 week after the second infusion), and completed six infusions by month 2.3. Patients 1, 3 and 6
392 only received NK cell therapy, whereas patients 2, 4 and 5 received additional treatment(s) as
393 indicated. Patient 1 exhibited progressive disease (PD) at month 2.7 and left the trial. Patient 2
394 displayed SD for 8.2 months, during which a partial response (PR) was detected at month 4.4.
395 She then received maintenance metronomic Endoxan starting from month 8.4, and displayed
396 SD or PR for a further 50 months. Patient 3 displayed SD for 52.7 months. Patient 4 exhibited
397 an SD state for 13 months, received Tarceva during months 14.9-18.6, suffered PD at month
398 18.6 that prompted receipt of other treatments, and ultimately left the trial at month 31.5.
399 Patient 5 presented SD for 9.9 months, and received metronomic Endoxan during months 7.7-
400 13.5, 28.9-33.0, and 43.6-46.1. She underwent ultrasound imaging during months 17.6-54.2
401 and the results support a continuing SD state. Patient 6 retained an SD state for 36.3 months,
402 and subsequent ultrasound imaging in month 44.5 supports a continuing SD state. In summary,
403 among the four patients with metastatic solid tumors, patients 1 and 4 exhibited PD at month
404 2.7 and 18.6, respectively, leaving the trial at months 2.7 and 31.5, respectively. In contrast,
405 patients 3 and 6, who only received NK cell therapy, exhibited a SD state and both survived
406 for 60 months. The two follicular lymphoma patients (patients 2 and 5) who started
407 maintenance Endoxan therapy ~6 months after undergoing the NK-cell therapy have exhibited
408 a SD state and both survived for 60 months. These preliminary results suggest some level of
409 effectiveness for the autologous NK cell therapy, supporting the efficacy of our pre-clinical
410 mouse model.

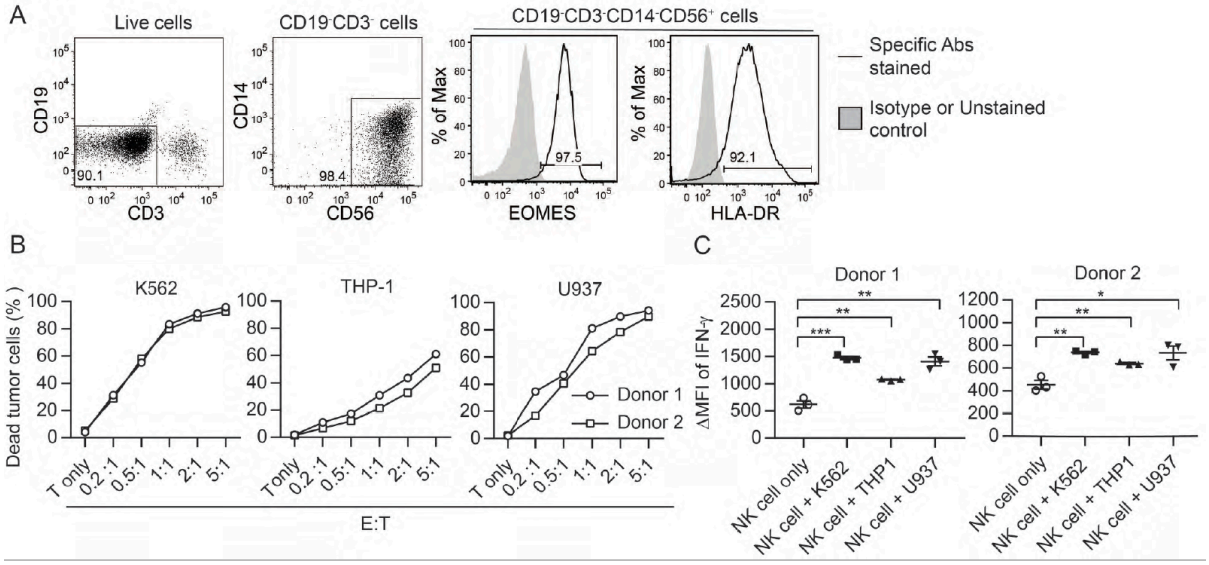

Figure 7. Ex vivo-expanded human NK cells exhibit anti-tumor activities in vitro.

(A) Analysis of expanded human NK cells. Live cells among total cells obtained from human PBMC culture (as described in Methods) were analyzed for the expression of indicated molecules by FACS. Representative plots of 33 healthy donors are shown. (B) Expanded human NK cells kill tumor cells in vitro. Sorted HLA-DR$^+$ NK cells from two healthy donors were co-cultured with CFSE-labeled tumor cells at the indicated E:T ratio. Percentage of dead tumor cells represents the mean ± SEM of PI$^+$ cells among CFSE$^+$ tumor cells from triplicate wells. (C) Expanded human NK cells up-regulate IFN-γ production in response to tumor cells in vitro. Sorted HLA-DR$^+$ NK cells from two healthy donors were co-cultured with tumor cells at a 1:1 ratio for 5 h. Levels of IFN-γ in NK cells were examined by intracellular staining and are calculated as the ΔMFI ± SEM between specific antibody-stained and isotype control antibody-stained samples. Statistical significance was determined by unpaired two-tailed Student's t-test: *P<0.05, **P<0.01, ***P<0.001 relative to NK cells only.

Table. Baseline characteristics of the patients enrolled in the phase I trial.

Characteristic	Cohort 1			Cohort 2		
Patient	1	2	3	4	5	6
Age	63	42	59	66	54	65
Gender	Male	Female	Female	Female	Female	Male
Primary cancer	Colon	Follicular lymphoma	Lung	Lung	Follicular lymphoma	Bladder
Metastasis	Adrenal Lung Pelvis		Lung	Brain		Bone
Previous therapies for cancer						
Surgery	Yes	No	Yes	Yes	No	Yes
Radiotherapy	No	No	No	Yes	No	No
Lines of chemo- or targeted therapy	1	3	0	3	2	4
Immunotherapy	No	No	No	No	No	Keytruda[a]
ECOG performance status	0	0	0	0	0	0
Target lesion (mm)	Pelvic LN (16.3)	Left inguinal LN (18.4)	Mediastinal LN (12.3)	Lung left upper lobe (6.4)	Left axillary LN (10.4)	Pelvic LN (22.7)

a: Ended 7 months before NK cell therapy

424

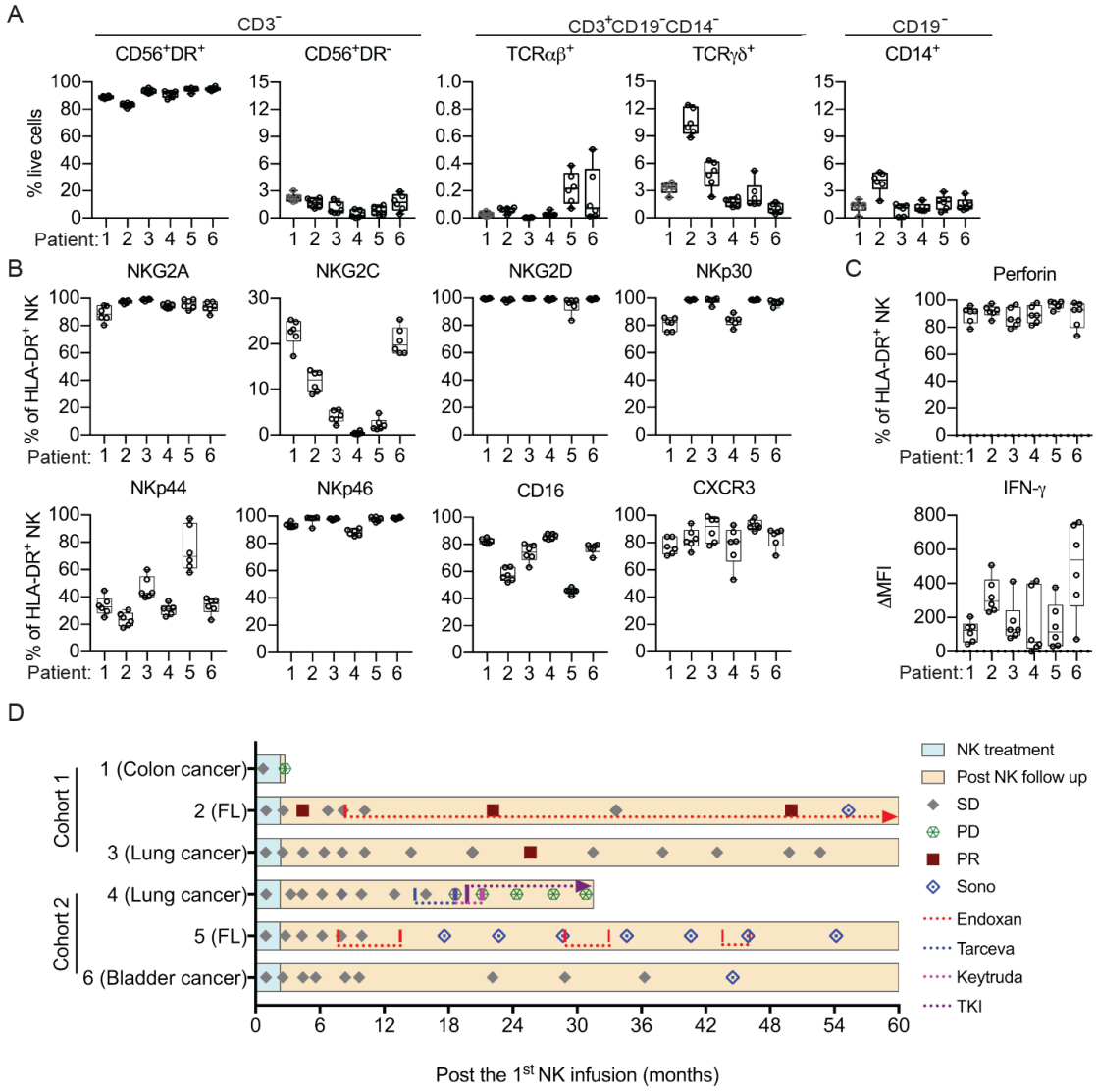

Figure 8. Clinical outcomes of autologous NK cell therapy.

(A) Composition of the infused cells for each patient over six batches of cell preparation. Expression of (B) NKRs, CD16 and CXCR3 and (C) perforin and IFN-γ by the expanded HLA-DR$^+$ NK cells over six batches of cell preparation. Each dot represents a batch of cell preparation. (D) Clinical responses and survival of the six patients. The blue and yellow blocks represent the durations of NK cell treatment and subsequent follow-up, respectively. The response of patients (SD, PD or PR) was evaluated by CT imaging according to RECIST 1.1. Sono symbol marks follow-up using ultrasound imaging. Colored dotted lines indicate the timeframes for additional medications.

Figure supplement 1. Expression of CD56 and HLA-DR by CD3$^-$CD19$^-$CD14$^-$ cells after *ex vivo* expansion (related to Figure 6A).

Figure supplement 2. Expression of NKRs, CD16 and CXCR3 by the expanded HLA-DR$^+$ NK cells.

Figure supplement 3. Expression of IFN-γ and perforin in the expanded HLA-DR$^+$ NK cells.

439 **Discussion**

440

441 The limited benefit achieved with adoptive autologous NK cell therapy for metastatic solid
442 tumors is paradoxical given the clear anti-tumor functions of endogenous NK cells. In this
443 study, we found that transfer of syngeneic NK cells conditioned using IL-15 and IL-12 after
444 resecting the primary tumor resulted in long-term survival of mice with low burden lung
445 metastases. Our results indicate a requirement for $CD8^+$ T cells and the contribution of $CD4^+$
446 T cells to the effectiveness of this NK cell therapy (Figure 3D), which is distinct from the T-
447 cell-independent anti-metastasis mechanisms of NK cells demonstrated previously (Correia et
448 al., 2021; Malladi et al., 2016; Mittal et al., 2017; Takeda et al., 2011; Uemura et al., 2010).
449 The difference in T cell dependency likely arises from differences in experimental design.
450 These previous studies examined the effect of endogenous NK cells on experimental metastasis
451 following intravenous or intrasplenic tumor cell injection by enumerating metastases of
452 affected organs 14 days later. Given that the effect of NK cells on experimental metastasis is
453 mediated by clearing intraluminal tumor cells in microvessels before they extravasate into the
454 target tissue (Spiegel et al., 2016), these studies assessed T cell-independent control of
455 metastasis by NK cells. In contrast, our study examined the effect of adoptively transferred ex
456 vivo-stimulated NK cells on spontaneous metastasis by measuring long-term survival, in which
457 lung metastases were established before primary tumor resection and NK cell administration
458 (Figure 2A). The T cell dependency of the NK cell therapy in our model indicates that innate
459 mechanisms are not sufficient to support the long-term survival of mice with EO771 metastases,
460 which is consistent with the finding from experimental metastasis models that NK cells alone
461 cannot reduce metastases after tumor cells have seeded the target tissue (Spiegel et al., 2016).
462 Importantly, the timeframe we adopted for measuring long-term survival covers the period for
463 the innate effect of the transferred NK cells and the effect of a full T cell response with memory.

464 The $CD8^+$ T cell dependency implies that the transferred NK cells act as an upstream controller
465 for an effective anti-tumor T cell response, which is in line with a previous study showing that
466 early intratumoral accumulation of IFN-γ-producing endogenous NK cells is required for $CD8^+$
467 T cell-mediated eradication of *Cox*-deficient melanoma in immunocompetent wild-type mice
468 (Bonavita et al., 2020).
469
470 In studying the mechanism underlying T cell-dependency for the effectiveness of NK cell
471 therapy, our results from a mouse model reveal that transfer of WT NK cells augments
472 activation of cDC1s and cDC2s in the metastatic lung (Figure 4). cDC1s and cDC2s present
473 cell-associated and soluble antigens, respectively, to $CD4^+$ and $CD8^+$ T cells (Hildner et al.,
474 2008). The increase of MHC-II^{hi} cDC subsets and elevated expression of MHC-I, MHC-II and
475 CD86 by lung cDC1s and cDC2s presumably promotes T cell activation, which is consistent
476 with the increase of activated lung $Foxp3^-CD4^+$ and $CD8^+$ T cells (Figure 5). Moreover, the
477 elevated CD40 expression by cDC1 and $CD4^+$ T cell activation implies cDC1-relayed $CD4^+$ T
478 cell help for $CD8^+$ T cell response in the lung (Ferris et al., 2020). We also detected an increase
479 of SCL $CD8^+$ T cells in metastatic lungs upon NK cell transfer (Figure 5D). Intratumoral
480 tumor-specific SCL $CD8^+$ T cells are known to mediate the responses to PD-1/PD-L1 blockade
481 and adoptive T cell immunotherapies (Krishna et al., 2020; Siddiqui et al., 2019) and are
482 supplied from a reservoir of precursors in the tumor dLN (Connolly et al., 2021; Schenkel et
483 al., 2021). As cDC1s in tumor dLN maintain the SCL $CD8^+$ T cell precursor reservoir
484 (Schenkel et al., 2021), the increase of migratory cDC1 in mLN upon NK cell transfer (Figure
485 6B) likely contribute to the increase of lung SCL $CD8^+$ T cells. Moreover, a recent study
486 reported that the SCL $CD8^+$ T cell precursors are activated by tumor antigens in the tumor dLN
487 and acquire a stem-like state without an effector phenotype (Prokhnevska et al., 2023). After
488 migrating to a tumor, they differentiate from SCL to an effector state, which requires

489 costimulation by CD80 and CD86 of APC in the TME (Prokhnevska et al., 2023). Our findings
490 of augmented CD86 expression by cDCs and increased proliferating SCL $CD8^+$ T cells in
491 response to NK-cell transfer in metastatic lung are in line with the two-step activation of
492 intratumoral SCL $CD8^+$ T cells. Together, these results demonstrate a clear association between
493 the activation of lung cDCs and T cells in response to NK cell transfer. Furthermore, IFN-γ of
494 transferred NK cells is essential for the activation of both cDCs and T cells, strengthening
495 evidence for the scenario that NK cells activate cDCs and then cDCs activate T cells. The
496 requirement for IFN-γ of transferred NK cells also suggests a direct interaction between
497 transferred NK cells and lung cDCs. The increase of $CCR7^+LAMP3^+$ MHC-II^{hi} cDCs supports
498 this supposition, with a recent study reporting colocalization of $LAMP3^+$ DCs with NK cells
499 in four types of human solid tumor (Tang et al., 2023). Moreover, this result indicates that NK-
500 cell-derived IFN-γ drives the generation of mregDCs.
501
502 In summary, our results indicate that syngeneic IL-15/IL-12-conditioned NK cell therapy
503 promotes tumor-specific T cell responses, at least in part, through activation of cDC1s and
504 cDC2s in metastatic lung. Our findings are consistent with the critical role of endogenous NK
505 cells and $CD8^+$ T cells in anti-tumor immunity, and support that autologous NK cell therapy is
506 effective in treating established low burden MHC-I^+ metastases by enhancing the tumor-
507 specific $CD8^+$ T cell response.
508
509
510 **Materials and Methods**
511
512 **Mice and cell lines**

513 Female C57BL/6JNarl mice (National Laboratory Animal Center of Taiwan, Taipei, Taiwan),
514 *eGFP* transgenic C57BL/6JNarl mice (a gift from Chin-Yen Tsai at Academia Sinica (AS)),
515 *Ifng*$^{-/-}$ mice (strain # 002287, The Jackson Laboratory, Bar Harbor, ME, USA) and *Il10*$^{-/-}$ mice
516 (Strain # 002251, The Jackson Laboratory) were housed in a specific pathogen-free animal
517 facility at the Institute of Molecular Biology. Mice aged 8-12 weeks old were used for
518 experiments, unless stated otherwise. All animal protocols were approved by the IACUC of
519 AS. EO771 (CH3 Biosystems), K562 (a gift from Che-Kun James Shen at AS), THP-1 and
520 U937 (gifts from Li-Chung Hsu at National Taiwan University) cells were cultured in RPMI-
521 1640 (Gibco, Grand Island, NY, USA) containing 10% FBS (Hyclone, Marlborough, MA,
522 USA), 20 mM HEPES (Sigma-Aldrich, St. Louis, MO, USA), 100 U/ml penicillin and 100
523 μg/ml streptomycin (Gibco). B16F10 melanoma (a gift from Steve Roffler at AS) was cultured
524 in DMEM (Gibco) containing 10% FBS and 100 U/ml penicillin and 100 μg/ml streptomycin.
525
526 **Flow cytometry**
527 To stain cell surface molecules, cells were incubated with fluorophore-conjugated antibodies
528 for 15 min at 4 °C and washed twice with staining buffer (PBS containing 2% FBS, 5 mM
529 EDTA and 0.01% NaN_3). For staining of intracellular molecules, cells were fixed for 30 min
530 at 4 °C after surface staining with 4% paraformaldehyde, or with a Foxp3/Transcription Factor
531 Fixation/Permeabilization Concentrate and Diluent kit (Thermo Fisher Scientific, Waltham,
532 MA, USA) to stain transcription factors. The fixed cells were then washed with staining buffer,
533 permeabilized with 0.1% saponin, and stained with antibody for 30 min at 4 °C. Cells were
534 analyzed by LSRII, FACSymphony A3 or FACSCalibur (BD Biosciences, Franklin Lakes, NJ,
535 USA) and the data were analyzed using FlowJo (BD Biosciences). The antibodies used are
536 detailed in the supplementary materials.
537

538 **Ex vivo expansion of murine and human NK cells**

539 Murine bone marrow (BM) cells were depleted of red blood cells (RBCs) by means of
540 ammonium-chloride-potassium (ACK) buffer (150 mM NH_4Cl, 10 mM $NaHCO_3$, 1 mM
541 EDTA) and then cultured in RPMI-1640 containing 10% FBS (Corning, Corning, NY, USA),
542 20 mM HEPES (Sigma-Aldrich), 200 U/ml penicillin, 200 μg/ml streptomycin (Gibco), 50
543 μg/ml gentamycin (Sigma-Aldrich), 0.2 mg/ml L-glutamine (Sigma-Aldrich), and 50 μM 2-
544 mercaptoethanol (Merck, Rahway, NJ, USA) in a 5% CO_2 incubator at 37 °C for 7 days with
545 30 ng/ml IL-15 (BioLegend, San Diego, CA, USA) and 10 ng/ml IL-12 (Peprotech, Cranbury,
546 NJ, USA). The expanded murine NK cells ($CD19^-TCR\beta^-NK1.1^+CD11c^+B220^+$) were sorted
547 using SORP (BD Biosciences). Human NK cells were expanded from peripheral blood
548 mononuclear cells (PBMCs) after depleting $TCR\beta^+$ and $CD19^+$ cells with anti-TCRβ (WT31,
549 BD Biosciences) and anti-CD19 (4G7, BD Biosciences) antibodies, and anti-mouse IgG1
550 microbeads (Miltenyi Biotec, Bergisch Gladbach, Germany) using an LD column with a
551 QuadroMACS Separator (Miltenyi Biotec) under good tissue practice (GTP) conditions. The
552 resulting $TCR\beta^-CD19^-$ PBMCs were cultured in RPMI-1640 containing autologous plasma, 20
553 mM HEPES (Sigma-Aldrich), 2 mM L-glutamine (Cellgro, Lincoln, NE, USA), and 50 μg/ml
554 gentamycin (Winston Medical Supply Co. Ltd.) in a 5% CO_2 incubator at 37 °C for 7 days with
555 25 ng/ml IL-15 (CellGenix, Freiburg, Germany) and 10 ng/ml IL-12 (BioLegend) (Lee & Liao,
556 2015).

557

558 **In vitro anti-tumor activity of expanded NK cells**

559 Tumor cells were labeled using a Vybrant CFDA SE (CFSE) cell tracer kit (Invitrogen,
560 Waltham, MA, USA). For cytotoxicity assay, sorted NK cells were co-cultured with 10^5
561 labeled tumor cells at the indicated ratio and then incubated for 5 h in a 5% CO_2 incubator at
562 37 °C. The cells were then stained with propidium iodide (PI) and the $CFSE^+$ tumor cells were

563 analyzed for PI^- cells using a LSRII system. For IFN-γ production, sorted NK cells were co-
564 cultured with CFSE-labeled tumor cells at a 1-to-1 ratio, with 10 μg/ml brefeldin A being
565 present for the last 4 h of the co-culture. Cells were then stained intracellularly with anti-IFN-
566 γ or isotype control antibody to detect IFN-γ production by $CFSE^-$ NK cells using a LSRII
567 system.
568
569 **Trafficking of ex vivo-expanded murine NK cells**
570 NK cells expanded from the BM cells of *eGFP* transgenic mice were sorted and intravenously
571 transferred into C57BL/6JNarl mice (6 million cells/mouse) 3 days after resection of a day-21
572 tumor. Single cell suspensions were prepared from the lung and spleen at the indicated hours
573 after NK cell transfer and analyzed for $eGFP^+$ donor cells using a LSRII system.
574
575 **Gene expression**
576 Lung RNA was extracted using Trizol (Invitrogen) and reverse-transcribed into cDNA using a
577 Reverse Transcription Kit (SMOBIO, Paramount, California, USA). Relative gene expression
578 was determined using a QuantStudio 12K Flex Real-Time PCR system (Thermo Fisher
579 Scientific) with SYBR Green and relative standard curves normalized against expression of
580 cyclophilin a (*Cypa*). The sequences of primers used are detailed in the supplementary
581 materials.
582
583 **EO771 resection and metastasis model and NK cell treatment**
584 Each mouse was inoculated with 0.3 million EO771 cells into the right fourth mammary fat
585 pad on day 0. Twenty-one days later, mice were anesthetized and the resulting tumor and
586 sentinel LN (right inguinal LN) were resected. Sham control mice received the same surgical
587 procedure without removing any tissue. Mice harboring a day-21 tumor weight of <95 mg were

588 excluded since resection alone promoted long-term survival of mice with such tumors. Mice
589 were grouped to have a similar mean and standard deviation of day-21 tumor weight. Each
590 mouse then received 0.3 million expanded NK cells or PBS (Control) via the tail vein three
591 times on days 24, 28 and 31, or once on day 24 as indicated. The resulting metastatic foci on
592 lung surfaces were visualized by staining the dissected lung with India ink under a dissecting
593 microscope. The area of metastatic foci was determined using ImageJ (NIH). For T cell
594 depletion, mice were administered intraperitoneally with 200 μg of anti-CD4 (GK1.5, BioXcell,
595 Lebanon, NH, USA), anti-CD8α (2.43, BioXcell), or both antibodies 19 days after EO771
596 inoculation, whereas control mice each received 400 μg of isotype control antibody (Rat IgG2b,
597 κ; BioXcell). The mice underwent tumor resection 2 days later, before receiving NK cells as
598 described in the previous section.
599
600 **Isolation of murine T cells and non-T cells**
601 Single cell suspensions were prepared from the BM, spleen, and LNs of NK cell-treated and
602 tumor-rechallenged long-term survivors and from the same tissues of age-matched naïve mice.
603 After lysis of RBCs with ACK buffer, T cells and non-T cells were isolated using Pan T cell
604 isolation Kit II (Miltenyi Biotec) via an autoMACS Pro Separator (Miltenyi Biotec) according
605 to the manufacturer's instructions. The T cell preparations comprised 88-93% of $CD3^+$ cells,
606 and the non-T cell preparations comprised 90-96% of $CD3^-$ cells.
607
608 **Preparation of lung cell suspension**
609 Each mouse received an intravenous injection of 3 μg of FITC-anti-CD45 antibody three
610 minutes before euthanasia to label blood $CD45^+$ cells. Lungs were harvested, minced and
611 washed with PBS to remove excess anti-CD45 antibody. The tissue pieces were digested with
612 0.2 μg/ml of collagenase IV in HBSS (Sigma H1641) containing 2% FBS and 10mM HEPES

613 for 30 min at 37°C with shaking at 200 rpm. RBCs in the lung cell suspension were lysed using
614 ACK lysis buffer.
615
616 **Clinical trial design**
617 We conducted an investigator-driven, open-label, 3+3 design trial to investigate the safety of
618 the autologous NK cell therapy on metastatic/refractory stage IV cancer patients at a single
619 center (ClinicalTrials.gov Identifier: NCT02661685). All six patients were ineligible for or
620 refused further systemic chemotherapy or immunotherapy, and had an Eastern Cooperative
621 Oncology Group (ECOG) performance status of 0, a target lesion, and adequate organ function
622 at the time of enrollment. The three patients in cohort 1 received six bi-weekly intravenous
623 infusions of 20×10^6 expanded autologous HLA-DR$^+$ NK cells, whereas the three patients in
624 cohort 2 were administered with 30×10^6 of the same cells. All patients underwent a
625 computerized tomography (CT) scan between the second and the third NK cell infusions, and
626 then five further CT scans at 8-week intervals starting one week after the sixth infusion.
627 Thereafter, CT or sonography scans were performed as indicated. Safety was evaluated by
628 assessing dose-limiting toxicity (DLT), defined as any treatment-related toxicity of grade 3 or
629 above of general or immune disorders according to the National Cancer Institute-Common
630 Terminology Criteria for Adverse Events (NCI-CTCAE) v4.03. Fever, chills, flu-like
631 symptoms, or infusion-related reactions of grade 3 or above were considered DLT only if they
632 remained at grade 3 or above for more than 3 days despite appropriate medication. Clinical
633 responses to the therapy were evaluated by CT scans according to Response Evaluation Criteria
634 in Solid Tumors version 1.1 (RECIST 1.1). Patient survival was followed every 8 weeks for
635 the first year and every 12 weeks from the second to the fifth year.
636
637 **Trial oversight**

638 The protocols for our clinical trial and follow-up were approved by the Institutional Review
639 Boards (IRBs) at Tri-Service General Hospital and at AS, and were conducted according to the
640 principles of the Declaration of Helsinki. Written informed consent was obtained from all
641 patients.
642
643 **Statistical analysis**
644 Results are presented as mean ± SEM. Statistical significance of in vitro cytotoxicity was
645 examined by unpaired two-tailed Student's t-test. Correlation was determined by Pearson
646 correlation coefficient. The Kaplan-Meier estimator was employed for survival analysis, and
647 statistical significance was determined by a Log-Rank test. Tumor volume was calculated using
648 the formula: length x width^2 x 0.52. Mice with a tumor volume exceeding 2000 mm^3 were
649 considered moribund. All statistical analyses were performed using GraphPad Prism 7
650 (GraphPad). ns, not significant; *P<0.05; **P<0.01; ***P<0.001; ****P<0.0001.
651
652
653 **Acknowledgments**
654 We thank the FACS Core and Animal Facilities at the Institute of Molecular Biology, AS, for
655 service and support. We thank Dr. Chee-Jen Chang at the Graduate Institute of Clinical Medical
656 Science, Chang Gung University, for consultation on statistical design of the clinical trial. We
657 thank Ms. Yi-Min Liu and colleagues at the Translation Resource Center for Genomic
658 Medicine, Institute of Biomedical Science, AS, for assistance with designing the case report
659 form, the Oracle clinical system and IRB affairs. We thank the Instrument Center at the
660 National Defense Medical Center for flow cytometry services. We thank Dr. John O'Brien for
661 manuscript editing.
662

663

664 **References**

665 Alspach, E., Lussier, D. M., & Schreiber, R. D. (2019). Interferon gamma and Its Important
666 Roles in Promoting and Inhibiting Spontaneous and Therapeutic Cancer Immunity.
667 *Cold Spring Harb Perspect Biol, 11*(3). doi:10.1101/cshperspect.a028480

668 Andreatta, M., Corria-Osorio, J., Muller, S., Cubas, R., Coukos, G., & Carmona, S. J. (2021).
669 Interpretation of T cell states from single-cell transcriptomics data using reference
670 atlases. *Nat Commun, 12*(1), 2965. doi:10.1038/s41467-021-23324-4

671 Barry, K. C., Hsu, J., Broz, M. L., Cueto, F. J., Binnewies, M., Combes, A. J., . . . Krummel,
672 M. F. (2018). A natural killer-dendritic cell axis defines checkpoint therapy-responsive
673 tumor microenvironments. *Nat Med, 24*(8), 1178-1191. doi:10.1038/s41591-018-0085-
674 8

675 Bonavita, E., Bromley, C. P., Jonsson, G., Pelly, V. S., Sahoo, S., Walwyn-Brown, K., . . .
676 Zelenay, S. (2020). Antagonistic inflammatory phenotypes dictate tumor fate and
677 response to immune checkpoint blockade. *Immunity, 53*(6), 1215-1229 e1218.
678 doi:10.1016/j.immuni.2020.10.020

679 Bottcher, J. P., Bonavita, E., Chakravarty, P., Blees, H., Cabeza-Cabrerizo, M., Sammicheli,
680 S., . . . Reis e Sousa, C. (2018). NK Cells Stimulate Recruitment of cDC1 into the
681 Tumor Microenvironment Promoting Cancer Immune Control. *Cell, 172*(5), 1022-
682 1037.e1014. doi:10.1016/j.cell.2018.01.004

683 Cabeza-Cabrerizo, M., Cardoso, A., Minutti, C. M., Pereira da Costa, M., & Reis e Sousa, C.
684 (2021). Dendritic Cells Revisited. *Annu Rev Immunol, 39*, 131-166.
685 doi:10.1146/annurev-immunol-061020-053707

686 Calagua, C., Ficial, M., Jansen, C. S., Hirz, T., Del Balzo, L., Wilkinson, S., . . . Einstein, D. J.
687 (2021). A Subset of Localized Prostate Cancer Displays an Immunogenic Phenotype

688 Associated with Losses of Key Tumor Suppressor Genes. *Clin Cancer Res, 27*(17),
689 4836-4847. doi:10.1158/1078-0432.CCR-21-0121
690 Castiglioni, A., Yang, Y., Williams, K., Gogineni, A., Lane, R. S., Wang, A. W., . . . Muller,
691 S. (2023). Combined PD-L1/TGFbeta blockade allows expansion and differentiation of
692 stem cell-like CD8 T cells in immune excluded tumors. *Nat Commun, 14*(1), 4703.
693 doi:10.1038/s41467-023-40398-4
694 Chen, X. H., Liu, Z. C., Zhang, G., Wei, W., Wang, X. X., Wang, H., . . . Du, J. (2015). TGF-
695 beta and EGF induced HLA-I downregulation is associated with epithelial-
696 mesenchymal transition (EMT) through upregulation of snail in prostate cancer cells.
697 *Mol Immunol, 65*(1), 34-42. doi:10.1016/j.molimm.2014.12.017
698 Cheng, S., Li, Z., Gao, R., Xing, B., Gao, Y., Yang, Y., . . . Zhang, Z. (2021). A pan-cancer
699 single-cell transcriptional atlas of tumor infiltrating myeloid cells. *Cell, 184*(3), 792-
700 809 e723. doi:10.1016/j.cell.2021.01.010
701 Chockley, P. J., Chen, J., Chen, G., Beer, D. G., Standiford, T. J., & Keshamouni, V. G. (2018).
702 Epithelial-mesenchymal transition leads to NK cell-mediated metastasis-specific
703 immunosurveillance in lung cancer. *J Clin Invest, 128*(4), 1384-1396.
704 doi:10.1172/JCI97611
705 Connolly, K. A., Kuchroo, M., Venkat, A., Khatun, A., Wang, J. W., William, I., . . . Joshi, N.
706 S. (2021). A reservoir of stem-like CD8 T cells in the tumor-draining lymph node
707 preserves the ongoing antitumor immune response. *Science Immunology, 6*(64).
708 doi:https://doi.org/10.1126/sciimmunol.abg7836
709 Correia, A. L., Guimaraes, J. C., Auf der Maur, P., De Silva, D., Trefny, M. P., Okamoto, R., . . .
710 Bentires-Alj, M. (2021). Hepatic stellate cells suppress NK cell-sustained breast cancer
711 dormancy. *Nature, 594*(7864), 566-571. doi:10.1038/s41586-021-03614-z

712 de Saint-Vis, B., Vincent, J., Vandenabeele, S., Vanbervliet, B., Pin, J. J., Ait-Yahia, S., . . .
713 Lebecque, S. (1998). A novel lysosome-associated membrane glycoprotein, DC-LAMP,
714 induced upon DC maturation, is transiently expressed in MHC class II compartment.
715 *Immunity, 9*(3), 325-336. doi:10.1016/s1074-7613(00)80615-9
716 Ewens, A., Mihich, E., & Ehrke, M. J. (2005). Distant metastasis from subcutaneously grown
717 E0771 medullary breast adenocarcinoma. *Anticancer Res, 25*(6b), 3905-3915.
718 Retrieved from http://ar.iiarjournals.org/content/25/6B/3905.full.pdf
719 Fang, F., Xiao, W., & Tian, Z. (2017). NK cell-based immunotherapy for cancer. *Semin*
720 *Immunol, 31*, 37-54. doi:10.1016/j.smim.2017.07.009
721 Ferris, S. T., Durai, V., Wu, R., Theisen, D. J., Ward, J. P., Bern, M. D., . . . Murphy, K. M.
722 (2020). cDC1 prime and are licensed by CD4(+) T cells to induce anti-tumour immunity.
723 *Nature, 584*(7822), 624-629. doi:10.1038/s41586-020-2611-3
724 Freud, A. G., Mundy-Bosse, B. L., Yu, J., & Caligiuri, M. A. (2017). The Broad Spectrum of
725 Human Natural Killer Cell Diversity. *Immunity, 47*(5), 820-833.
726 doi:10.1016/j.immuni.2017.10.008
727 Ganesh, K., & Massague, J. (2021). Targeting metastatic cancer. *Nat Med, 27*(1), 34-44.
728 doi:10.1038/s41591-020-01195-4
729 Gordon, S. M., Chaix, J., Rupp, L. J., Wu, J., Madera, S., Sun, J. C., . . . Reiner, S. L. (2012).
730 The transcription factors T-bet and Eomes control key checkpoints of natural killer cell
731 maturation. *Immunity, 36*(1), 55-67. doi:10.1016/j.immuni.2011.11.016
732 Hildner, K., Edelson, B. T., Purtha, W. E., Diamond, M., Matsushita, H., Kohyama, M., . . .
733 Murphy, K. M. (2008). Batf3 deficiency reveals a critical role for CD8alpha+ dendritic
734 cells in cytotoxic T cell immunity. *Science, 322*(5904), 1097-1100.
735 doi:10.1126/science.1164206

736 Huntington, N. D., Cursons, J., & Rautela, J. (2020). The cancer-natural killer cell immunity
737 cycle. *Nat Rev Cancer, 20*(8), 437-454. doi:10.1038/s41568-020-0272-z
738 Jamieson, A. M., Diefenbach, A., McMahon, C. W., Xiong, N., Carlyle, J. R., & Raulet, D. H.
739 (2002). The role of the NKG2D immunoreceptor in immune cell activation and natural
740 killing. *Immunity, 17*(1), 19-29. doi:10.1016/s1074-7613(02)00333-3
741 Karre, K., Ljunggren, H. G., Piontek, G., & Kiessling, R. (2005). Selective rejection of H-2-
742 deficient lymphoma variants suggests alternative immune defence strategy. 1986. *J*
743 *Immunol, 174*(11), 6566-6569. Retrieved from
744 https://www.ncbi.nlm.nih.gov/pubmed/15905492
745 Kennedy, M. K., Glaccum, M., Brown, S. N., Butz, E. A., Viney, J. L., Embers, M., . . . Peschon,
746 J. J. (2000). Reversible defects in natural killer and memory CD8 T cell lineages in
747 interleukin 15-deficient mice. *J Exp Med, 191*(5), 771-780. doi:10.1084/jem.191.5.771
748 Krishna, S., Lowery, F. J., Copeland, A. R., Bahadiroglu, E., Mukherjee, R., Jia, L., . . .
749 Rosenberg, S. A. (2020). Stem-like CD8 T cells mediate response of adoptive cell
750 immunotherapy against human cancer. *Science, 370*(6522), 1328-1334.
751 doi:10.1126/science.abb9847
752 Lee, J. M., & Liao, N. S. (2015). United States Patent No. 9157068 B2.
753 Lodolce, J. P., Boone, D. L., Chai, S., Swain, R. E., Dassopoulos, T., Trettin, S., & Ma, A.
754 (1998). IL-15 receptor maintains lymphoid homeostasis by supporting lymphocyte
755 homing and proliferation. *Immunity, 9*(5), 669-676. doi:10.1016/s1074-
756 7613(00)80664-0
757 Lopez-Soto, A., Gonzalez, S., Smyth, M. J., & Galluzzi, L. (2017). Control of Metastasis by
758 NK Cells. *Cancer Cell, 32*(2), 135-154. doi:10.1016/j.ccell.2017.06.009
759 Lopez-Soto, A., Huergo-Zapico, L., Galvan, J. A., Rodrigo, L., de Herreros, A. G., Astudillo,
760 A., & Gonzalez, S. (2013). Epithelial-mesenchymal transition induces an antitumor

761 immune response mediated by NKG2D receptor. *J Immunol, 190*(8), 4408-4419.
762 doi:10.4049/jimmunol.1202950
763 Maier, B., Leader, A. M., Chen, S. T., Tung, N., Chang, C., LeBerichel, J., . . . Merad, M.
764 (2020). A conserved dendritic-cell regulatory program limits antitumour immunity.
765 *Nature, 580*(7802), 257-262. doi:10.1038/s41586-020-2134-y
766 Malladi, S., Macalinao, D. G., Jin, X., He, L., Basnet, H., Zou, Y., . . . Massague, J. (2016).
767 Metastatic Latency and Immune Evasion through Autocrine Inhibition of WNT. *Cell,*
768 *165*(1), 45-60. doi:10.1016/j.cell.2016.02.025
769 Marcenaro, E., Della Chiesa, M., Bellora, F., Parolini, S., Millo, R., Moretta, L., & Moretta, A.
770 (2005). IL-12 or IL-4 prime human NK cells to mediate functionally divergent
771 interactions with dendritic cells or tumors. *J Immunol, 174*(7), 3992-3998.
772 doi:10.4049/jimmunol.174.7.3992
773 Martin-Fontecha, A., Thomsen, L. L., Brett, S., Gerard, C., Lipp, M., Lanzavecchia, A., &
774 Sallusto, F. (2004). Induced recruitment of NK cells to lymph nodes provides IFN-
775 gamma for T(H)1 priming. *Nat Immunol, 5*(12), 1260-1265. doi:10.1038/ni1138
776 Martinez-Usatorre, A., Carmona, S. J., Godfroid, C., Yacoub Maroun, C., Labiano, S., &
777 Romero, P. (2020). Enhanced Phenotype Definition for Precision Isolation of Precursor
778 Exhausted Tumor-Infiltrating CD8 T Cells. *Front Immunol, 11*, 340.
779 doi:10.3389/fimmu.2020.00340
780 Melaiu, O., Lucarini, V., Cifaldi, L., & Fruci, D. (2019). Influence of the Tumor
781 Microenvironment on NK Cell Function in Solid Tumors. *Front Immunol, 10*, 3038.
782 doi:10.3389/fimmu.2019.03038
783 Mempel, T. R., Henrickson, S. E., & von Andrian, U. H. (2004). T-cell priming by dendritic
784 cells in lymph nodes occurs in three distinct phases. *Nature, 427*(6970), 154-159.
785 doi:10.1038/nature02238

786 Mittal, D., Vijayan, D., Putz, E. M., Aguilera, A. R., Markey, K. A., Straube, J., . . . Smyth, M.
787 J. (2017). Interleukin-12 from CD103(+) Batf3-dependent dendritic cells required for
788 NK-Cell suppression of metastasis. *Cancer Immunol Res, 5*(12), 1098-1108.
789 doi:10.1158/2326-6066.CIR-17-0341
790 Mocikat, R., Braumuller, H., Gumy, A., Egeter, O., Ziegler, H., Reusch, U., . . . Rocken, M.
791 (2003). Natural killer cells activated by MHC class I(low) targets prime dendritic cells
792 to induce protective CD8 T cell responses. *Immunity, 19*(4), 561-569. Retrieved from
793 https://ac.els-cdn.com/S1074761303002644/1-s2.0-S1074761303002644-
794 main.pdf?_tid=1a97a508-b220-482d-b58b-
795 ff113e2c772d&acdnat=1547709680_420dfea0f64bd7bf375b970454538332
796 Parkhurst, M. R., Riley, J. P., Dudley, M. E., & Rosenberg, S. A. (2011). Adoptive transfer of
797 autologous natural killer cells leads to high levels of circulating natural killer cells but
798 does not mediate tumor regression. *Clin Cancer Res, 17*(19), 6287-6297.
799 doi:https://doi.org/10.1158/1078-0432.CCR-11-1347
800 Prokhnevska, N., Cardenas, M. A., Valanparambil, R. M., Sobierajska, E., Barwick, B. G.,
801 Jansen, C., . . . Kissick, H. (2023). CD8+T cell activation in cancer comprises an initial
802 activation phase in lymph nodes followed by effector differentiation within the tumor.
803 *Immunity, 56*(1), 107-124.e105. doi:10.1016/j.immuni.2022.12.002
804 Raulet, D. H. (2003). Roles of the NKG2D immunoreceptor and its ligands. *Nat Rev Immunol,*
805 *3*(10), 781-790. doi:10.1038/nri1199
806 Riol-Blanco, L., Sánchez-Sánchez, N., Torres, A., Tejedor, A., Narumiya, S., Corbí, A. L., . . .
807 Rodríguez-Fernández, J. L. (2005). The chemokine receptor CCR7 activates in
808 dendritic cells two signaling modules that independently regulate chemotaxis and
809 migratory speed. *Journal of Immunology, 174*(7), 4070-4080. doi:DOI
810 10.4049/jimmunol.174.7.4070

811 Sakamoto, N., Ishikawa, T., Kokura, S., Okayama, T., Oka, K., Ideno, M., . . . Yoshikawa, T.
812 (2015). Phase I clinical trial of autologous NK cell therapy using novel expansion
813 method in patients with advanced digestive cancer. *J Transl Med, 13*, 277.
814 doi:10.1186/s12967-015-0632-8
815 Schenkel, J. M., Herbst, R. H., Canner, D., Li, A., Hillman, M., Shanahan, S. L., . . . Jacks, T.
816 (2021). Conventional type I dendritic cells maintain a reservoir of proliferative tumor-
817 antigen specific TCF-1 CD8 T cells in tumor-draining lymph nodes. *Immunity, 54*(10),
818 2338-2353.e2336. doi:10.1016/j.immuni.2021.08.026
819 Sharpe, A. H., & Pauken, K. E. (2018). The diverse functions of the PD1 inhibitory pathway.
820 *Nat Rev Immunol, 18*(3), 153-167. doi:10.1038/nri.2017.108
821 Siddiqui, I., Schaeuble, K., Chennupati, V., Marraco, S. A. F., Calderon-Copete, S., Ferreira,
822 D. P., . . . Held, W. (2019). Intratumoral Tcf1 PD-1 CD8 T Cells with Stem-like
823 Properties Promote Tumor Control in Response to Vaccination and Checkpoint
824 Blockade Immunotherapy. *Immunity, 50*(1), 195-221.e110.
825 doi:10.1016/j.immuni.2018.12.021
826 Smyth, M. J., Cretney, E., Kelly, J. M., Westwood, J. A., Street, S. E., Yagita, H., . . . Hayakawa,
827 Y. (2005). Activation of NK cell cytotoxicity. *Mol Immunol, 42*(4), 501-510.
828 doi:10.1016/j.molimm.2004.07.034
829 Spiegel, A., Brooks, M. W., Houshyar, S., Reinhardt, F., Ardolino, M., Fessler, E., . . .
830 Weinberg, R. A. (2016). Neutrophils suppress intraluminal NK Cell-mediated tumor
831 cell clearance and enhance extravasation of disseminated carcinoma cells. *Cancer*
832 *Discov, 6*(6), 630-649. doi:10.1158/2159-8290.CD-15-1157
833 Takeda, K., Nakayama, M., Sakaki, M., Hayakawa, Y., Imawari, M., Ogasawara, K., . . . Smyth,
834 M. J. (2011). IFN-gamma production by lung NK cells is critical for the natural

835 resistance to pulmonary metastasis of B16 melanoma in mice. *J Leukoc Biol, 90*(4),
836 777-785. doi:10.1189/jlb.0411208
837 Tang, F., Li, J. H., Qi, L., Liu, D. F., Bo, Y. F., Qin, S. S., . . . Zhang, Z. M. (2023). A pan-
838 cancer single-cell panorama of human natural killer cells. *Cell, 186*(19), 4235-
839 4251.e4220. doi:10.1016/j.cell.2023.07.034
840 Thommen, D. S., & Schumacher, T. N. (2018). T Cell Dysfunction in Cancer. *Cancer Cell,*
841 *33*(4), 547-562. doi:10.1016/j.ccell.2018.03.012
842 Uemura, A., Takehara, T., Miyagi, T., Suzuki, T., Tatsumi, T., Ohkawa, K., . . . Hayashi, N.
843 (2010). Natural killer cell is a major producer of interferon gamma that is critical for
844 the IL-12-induced anti-tumor effect in mice. *Cancer Immunol Immunother, 59*(3), 453-
845 463. doi:10.1007/s00262-009-0764-x
846 Yang, Y., Yang, H. H., Hu, Y., Watson, P. H., Liu, H. Y., Geiger, T. R., . . . Wakefield, L. M.
847 (2017). Immunocompetent mouse allograft models for development of therapies to
848 target breast cancer metastasis. *Oncotarget, 8*(19), 30621-30643.
849 doi:https://doi.org/10.18632/oncotarget.15695
850 Yang, Z. Z., Kim, H. J., Villasboas, J. C., Chen, Y. P., Price-Troska, T., Jalali, S., . . . Ansell,
851 S. M. (2017). Expression of LAG-3 defines exhaustion of intratumoral PD-1(+) T cells
852 and correlates with poor outcome in follicular lymphoma. *Oncotarget, 8*(37), 61425-
853 61439. doi:10.18632/oncotarget.18251
854